Improved representation of soil moisture ~~simulations~~ processes through incorporation of cosmic-ray neutron count measurements in a large-scale hydrologic model

Eshrat Fatima[1,2], Rohini Kumar[1], Sabine Attinger[1,2], Maren Kaluza[1], Oldrich Rakovec[1,3], Corinna Rebmann[1], Rafael Rosolem[4], Sascha Oswald[2], Luis Samaniego[1,2], Steffen Zacharias[5], and Martin Schrön[5]

[1]Dep. Computational Hydrosystems, UFZ - Helmholtz Centre for Environmental Research GmbH, Leipzig, Germany
[2]Institute of Environmental Science and Geography, University of Potsdam, Potsdam, Germany
[3]Faculty of Environmental Sciences, Czech University of Life Sciences Prague, Praha-Suchdol 16500, Czech Republic
[4]Department of Civil Engineering, University of Bristol, Bristol
[5]Dep. Monitoring and Exploration Technologies, UFZ - Helmholtz Centre for Environmental Research GmbH, Leipzig, Germany

Correspondence: Eshrat Fatima (eshrat.fatima@uni-potsdam.de), Rohini Kumar (rohini.kumar@ufz.de), Martin Schrön (martin.schroen@ufz.de)

Abstract. Profound knowledge of soil moisture and its variability plays a crucial role in hydrological modeling to support agricultural management, flood and drought monitoring and forecasting, and groundwater recharge estimation. Cosmic-ray neutron sensing (CRNS) ~~have~~ has been recognized as a promising tool for soil moisture monitoring due to ~~their~~ its hectare-scale footprint and decimeter-scale measurement depth. Different approaches ~~exists~~ exist that could be the basis for incorporating CRNS data into distributed hydrologic models, but largely still need to be implemented, thoroughly compared, and tested across different soil and vegetation types. This study establishes a framework to accommodate neutron count measurements and assess the accuracy of soil water content simulated by the mesoscale Hydrological Model (mHM) for the first time. It covers CRNS observations across different vegetation types in Germany ranging from agricultural areas to forest. We include two different approaches to estimate CRNS neutron counts in mHM based on the simulated soil moisture: a method based on the Desilets equation and another one based on the Cosmic-ray Soil Moisture Interaction Code (COSMIC). Within the Desilets approach, we further test two different averaging methods for the vertically layered soil moisture, namely uniform vs. non-uniform weighting scheme depending on the CRNS penetrating depth. ~~A Monte Carlos simulation with~~ We use a Monte Carlo simulation method, specifically the Latin hypercube sampling approach ~~(with N~~ with a large sample size (S = 100 000) ~~is employed~~ to explore and constrain the (behavioral) mHM parameterizations against observed CRNS neutron counts. Overall, the three methods perform well with Kling-Gupta efficiency > 0.8 and percent bias $< 1\%$ across the majority of investigated sites. We find that the non-uniform weighting scheme in the Desilets method ~~provide~~ and COSMIC method provides the most reliable performance, whereas the more commonly used approach with uniformly weighted average soil moisture overestimates the observed CRNS neutron counts. We then also demonstrate the usefulness of incorporating CRNS measurements into mHM for the simulations of both soil moisture and evapotranspiration and add a broader discussion on the potential and guidelines of incorporating CRNS measurements in large-scale hydrological and land surface models.

1 Introduction

Soil moisture is a key terrestrial climate variable because it controls the mass and energy exchange between the Earth's surface, the groundwater, the vegetation, and the atmosphere. Understanding soil moisture levels with changes in temperature is crucial for enhancing the predictability of climate patterns on inter-seasonal and annual time scales, as highlighted in previous studies (Santanello Jr et al., 2011; Seneviratne et al., 2006). Moreover, soil moisture variability also plays a significant role in a wide range of applications, including flood forecasting, weather forecasting, climate modeling, agricultural management, and groundwater recharge (Van Steenbergen and Willems, 2013; Albergel et al., 2010; Jablonowski, 2004; Wahbi et al., 2018; Samaniego et al., 2019; Barbosa et al., 2021). In hydrological modeling, soil moisture is a key variable controlling the partitioning of precipitation into evapotranspiration, infiltration, and runoff (Fuamba et al., 2019; Zhuo et al., 2020). Proper initialization and modeling of soil moisture are crucial for predicting other hydrologic processes (e.g., runoff, evapotranspiration, etc). ~~However~~Nevertheless, uncertainties in input data and model parameters, ~~and~~ along with limitations in the representation of subsurface processes, can impede the reliability of soil moisture estimation (Chen et al., 2011).

Obtaining accurate soil moisture measurements at a field scale is challenging due to ~~the limitations of current measurement methods and the complexity of subsurface processes~~ current measurement limitations and subsurface complexity (Dong and Ochsner, 2018). Estimating ~~the~~ average soil moisture at a mesoscale ($\approx$ 1–100 km) is particularly difficult ~~because of the limitations of current measurement techniques~~ due to measurement technique limitations in terms of their ~~measurement area or "footprint"~~ "footprint" and measurement methods ~~bridging~~ to bridge the scale gap between point-scale ~~measurements and the areal average required~~ and areal average measurements for hydrologic modeling ~~are needed~~ (Chan et al., 2018). One ~~of the promising approaches~~ promising approach to infer soil moisture at a field scale is ~~based on the recent development of a~~ the cosmic-ray neutron sensing (CRNS) technique (Zreda et al., 2008; Desilets et al., 2010; Köhli et al., 2015; Schrön et al., 2017). ~~The CRNS method utilizes naturally occurring neutrons on the Earth's surface produced by cosmic rays to derive near-surface soil moisture. The rate of neutron moderation in soil, and emitted neutron density above ground, is affected by soil moisture levels: dry soils emit more neutrons while wet soils moderate neutrons more strongly and emit less. This change in neutron emission can be detected with a neutron detector (Zreda et al., 2012b; Köhli et al., 2021). A cosmic-ray soil moisture probe is usually calibrated locally using soil samples from its support volume (Franz et al., 2012b; Schrön et al., 2017). CRNS has demonstrated a high potential for estimating average soil moisture over areas of several hectares in size and tens of decimeters in-depth (Köhli et al., 2015; Schrön et al., 2017). CRNS data are used in various studies like land surface modeling, understanding vegetation dynamics, catchment hydrology, and supporting the agriculture sector with information on soil types and climates (Franz et al., 2020). Soil moisture measured by CRNS has also been used in water balance studies and has been helpful in estimating infiltration and evapotranspiration (Schreiner-McGraw et al., 2015; Foolad et al., 2017; Wang et al., 2018).~~

Previous studies, such as Barbosa et al. (2021) and Brunetti et al. (2019)~~have~~, have recognized the importance of CRNS over traditional invasive point-scale techniques and have utilized the HYDRUS-1D model to simulate soil moisture at the field scale~~, incorporating the so-called~~. HYDRUS-1D offers a valuable framework for modeling soil moisture dynamics and has

been particularly addressing the subsurface processes. The studies incorporated a COSMIC operator to simulate neutron count rates of a CRNS measurement (Shuttleworth et al., 2013). They inversely calibrated soil hydraulic parameters by comparing observed and simulated neutron count rates, whereas beforehand this was limited to be done via comparison of depth-averaged soil moisture values (Rivera Villarreyes et al., 2014). The potential utility of using CRNS data to calculate volumetric soil water content (SWC) and improve soil hydraulic parameters within land surface models has also been observed earlier, as highlighted by Rosolem et al. (2014). Furthermore, depth-weighting schemes and hydrogen pools' effects on measurement depth revealed valuable insights. Shallow wetting fronts in sandy soils significantly impact measurement depth Franz et al. (2012a). Baroni and Oswald (2015) assessed three weighting techniques, resulting in depths varying from 23 to 28 cm, optimal estimates were achieved using vertically varying weights and considering additional hydrogen pools. In Iwema et al. (2017), a Land Surface Model investigated the impact of reducing scale mismatch between energy flux and soil moisture observations using CRNS data. Patil et al. (2021) employed a distributed Land Surface Model, Data Assimilation Research Testbed (DART) with CRNS time series, and Ensemble Adjustment Kalman Filter to simulate water and energy balance. Both studies focused on analyzing land surface water and energy balance, exploring data assimilation and calibration techniques.

The Hydrologiska Bryans Vattenbalansavdelning (HBV) model, as studied by Dimitrova-Petrova et al. (2020), employed CRNS data in a mixed-agricultural landscape to explore water balance on the land surface. While, Beck et al. (2021) used remote sensing products and groundwater level measurements to temporally calibrate the HBV model, emphasizing the challenge of comparing satellite-derived soil moisture with point-scale in-situ measurements. Additionally, Baatz et al. (2017) was the first study that utilized spatially distributed hydrological modeling, integrating CRNS data, FAO and BK50 soil maps, and other soil data in the Community Land Model (CLM). They demonstrated that assimilating CRNS data improved catchment-scale soil water content characterization by updating spatially distributed soil hydraulic parameters. Furthermore, Zhao et al. (2021) assessed the significance of CRNS data in CLM version 3.5, conducting simulations based on 13 CRNS stations over (2017-2018). Despite employing a simplified Richards equation, limitations included the absence of lateral flows and groundwater representation.

The mesoscale Hydrological Model (Samaniego et al., 2010b; Kumar et al., 2013b, mHM;) is known for its spatially distributed hydrologic predictions at a large scale incorporating scale-aware regionalized parameterization technique.

90 Therefore, by including a CRNS neutron count framework, the mHM model becomes a useful tool for improving simulated soil water content and furthering our understanding of the water cycle. This is made possible by the availability of observed CRNS data, which opens up new opportunities for research into novel hypotheses, improving model performance, and developing hydrological modeling methods. All the mentioned studies either compared the simulated and observed soil moisture products or incorporated the first COSMIC version to compare neutron counts directly. As argued by Shuttleworth et al. (2013), the

95 usage of neutron counts is the favorable way to compare simulations with data, since the CRNS sensor intrinsically averages over soil moisture layers while the measurement depth varies with soil moisture and consequently over time. Hence, the direct usage of CRNS neutron counts avoids the question of which modeled SWC layer the observations should be compared to and at what time scales. The COSMIC method ~~is complex because its approach enables a more~~ enables a comprehensive representation of the neutron ~~counting~~ generation process, which is computationally more demanding than using ~~the analytical~~

100 ~~Desilets equation (Desilets et al., 2010).~~ an analytical formulation (e.g., Desilets et al., 2010; Köhli et al., 2021).

In this study, we ~~incorporate the prediction of neutron counts directly within mHM .~~ established a framework to incorporate CRNS data into the mesoscale Hydrological Model (mHM) to compare empirical and physics-based approaches for neutron count estimation to improve soil water content parameters in mHM across different vegetation types in Germany. To do this, we compared modelled with measured neutron counts to infer soil hydraulic parameters. Here, we test three approaches, (i)

105 the direct calculation of neutrons from the equal-averaged SWC profiles based on Desilets et al. (2010), (ii) the same with a weighted-average profile SWC based on Schrön et al. (2017), and (iii) the physics-based model COSMIC by Shuttleworth et al. (2013). We evaluate the simulation of neutron counts at scales of ~~$1.2 \times 1.2 \, km^2$~~ $1.2 \, km \times 1.2 \, km$, comparing the results to observed neutron counts from three different sites including agriculture, deciduous forests, and grasslands. The goal of this study is to investigate the potential of using CRNS probes and measured neutron counts to improve soil moisture predictions

110 through simulations in mHM across different land covers and soil properties and to evaluate the feasibility of incorporating neutron count measurements into the modeling scheme. We employ a (calibration) framework by applying a Monte Carlo experiment to account for parameter uncertainties. We further cross-evaluate our simulations and test the reliability of the CRNS incorporated soil-moisture scheme in mHM for simulating other variables by utilising ~~time-series~~ time series of observed evapotranspiration from an eddy covariance station available. Finally, we discuss and provide guidelines (challenges

115 and limitations) for incorporating CRNS measurements in a large-scale hydrologic model.

In summary, the present paper aims to answer the following research questions:

- What is the best approach to simulate CRNS neutron counts in a hydrological model considering the heterogeneity of vertical soil moisture profiles?

- What is the impact of model calibration with CRNS observations on simulated ~~soil moisture and evapotranspiration~~

120 evapotranspiration at Hohes Holz?

- Is the mHM at approx. 1 km resolution capable of capturing the dynamics of hectare-scale CRNS measurements at different landcover sites in a grid including 2 agriculture sites, 1 forest site, and 1 meadow site?

2 Materials and Methods

2.1 Experimental Site Description

125 For this study, we select four sites with CRNS sensors, namely *Grosses Bruch*, *Hohes Holz*, *Hordorf*, and *Cunnersdorf* in Northern Germany, as provided already within COSMOS EU (Bogena et al., 2022) with particularly long time series and ~~homogeneous land cover~~with different land cover, i.e., agriculture, forest, and meadow (see Tab. 1). The first three sites belong to the TERENO observatory "Harz/Central Germany lowland" (Zacharias et al., 2011) while the fourth site is part of an agricultural research farm operated by the German Weather Service (DWD). The *Grosses Bruch* site is a meadow/grassland

130 that is usually flooded naturally once or twice a year~~and is thus prone to producing methane fluxes~~. The meadows have sandy loam fluvisol-gleysol soil, which is 1.5 meters deep and partially covered with a layer of peat (Wollschläger et al., 2017). Meteorological conditions like soil moisture and temperature at various depths are continuously monitored by a wireless soil moisture monitoring network (Schrön, 2017). *Hohes Holz* is a deciduous forest site and the performance of the CRNS sensor there is highly dependent on dynamic effects such as tree canopy water or seasonal fluctuations in wet biomass. Water trapped

135 in leaves and litter can present a particular challenge for CRNS measurements, especially at forest stations (Bogena et al., 2013). Also, Bogena et al. (2022) indicated that the influence of seasonal changes of biomass on the CRNS signal is much less important than the influence of changing soil moisture, even in Hohes Holz, as changes in soil moisture are the much larger source of variation represented by the CRNS measurements. The mean annual air temperature for each ~~sites~~ site ranges from 10.0 to 10.9 °C and the average yearly precipitation ranges from 458 to 535 mm.

Table 1. Geographical characteristics of study sites: Site Names, Geographic Coordinates, Climatic Data (Annual Precipitation in mm/year, Annual Mean Temperature in °C), and the Periods Covered in Observed and Simulated Datasets.

Site	Latitude	Longitude	Altitude	Land Cover	Precipitation	Temperature	Period
	[°N]	[°E]	[m]		[mm/year]	[°C]	
Grosses Bruch	52.02	11.10	80	Pasture, grassland	458	10.1	24/06/2014–31/01/2021
Hohes Holz	52.09	11.22	217	Forest, hilltop	469	10.3	27/08/2014–31/01/2021
Hordorf	51.99	11.17	82	Cropland	463	10.3	29/09/2016–31/01/2021
Cunnersdorf	51.36	12.55	140	Cropland	535	10.9	23/06/2016–31/01/2021
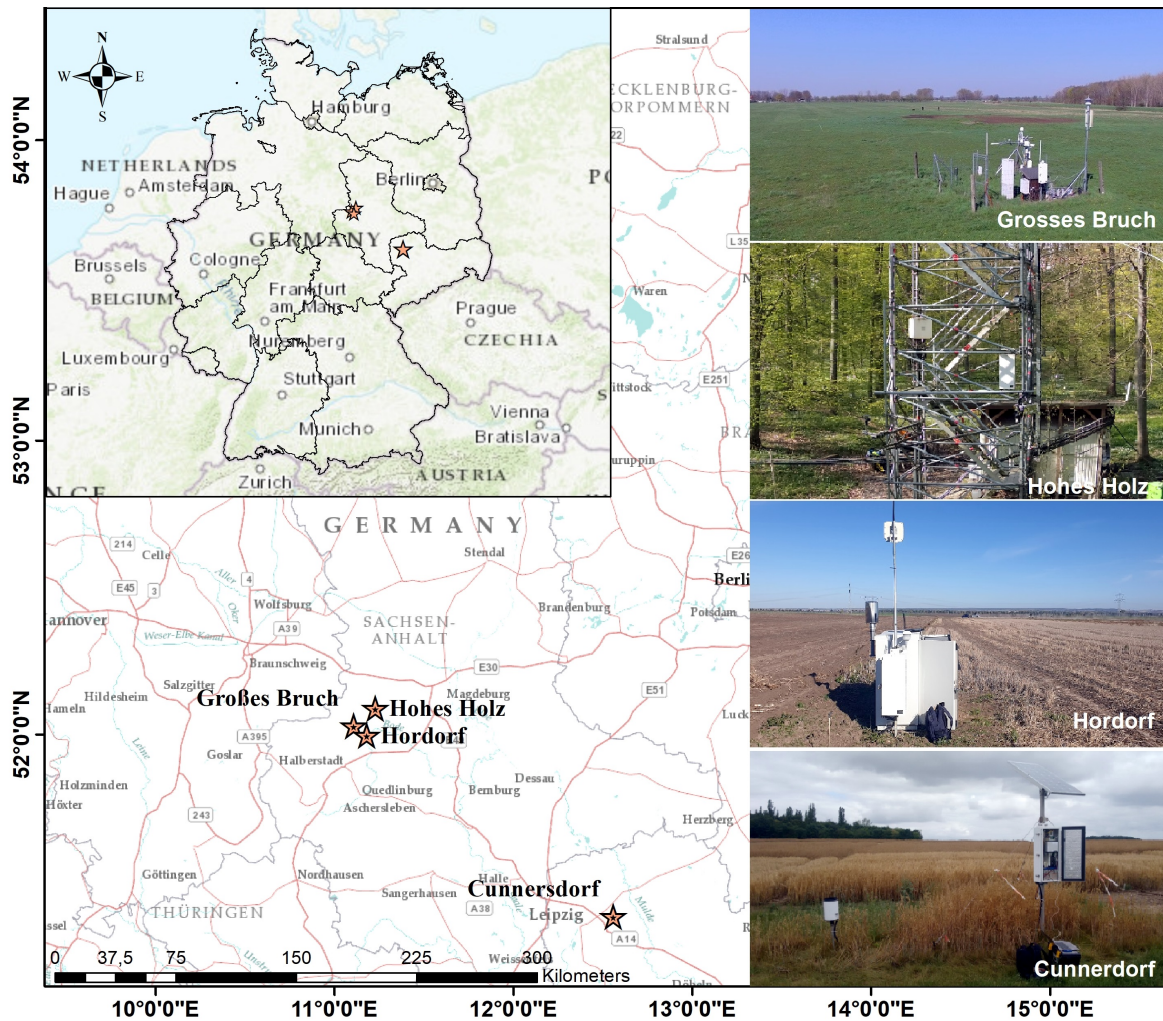
Figure 1. Study area map of Germany, highlighting the four test sites where observed neutron count rates from CRNS are utilized to evaluate the performance of mHM. The figure utilizes OSM basemap layers from (© OpenStreetMap contributors 2021; distributed under the Open Data Commons Open Database License (ODbL) v1.0) OpenStreetMap contributors (2020).

2.2 The mesoscale Hydrological Model (mHM)

mHM is a spatially distributed process-based hydrologic model (www.ufz.de/mhm) representing processes such as canopy interception, snow accumulation and melting, soil moisture dynamics, infiltration and surface runoff, evaporation, underground storage, and runoff generation, deep infiltration and baseflow, as well as runoff attenuation and flood routing (Samaniego et al., 2010a; Kumar et al., 2013a). The mHM model is flexible for hydrological simulations at different spatial scales due to its novel Multi-scale Parameter Regionalization approach (MPR; Samaniego et al., 2010b); and has demonstrated applicability in

140

145

diverse settings (Samaniego et al., 2010a; Kumar et al., 2013a; Rakovec et al., 2016; Samaniego et al., 2017). The MPR's basic concept is to estimate parameters (e.g., porosity) based on soil properties (e.g., sand and clay content) using transfer functions at a fine spatial resolution (e.g. 100 m) and upscaling them to modelling resolutions (e.g., 1 km). In MPR, transfer functions (e.g., pedo-transfer functions to estimate soil parameters) are combined with morphological inputs (e.g., soil texture properties) and

150   thus lead to model hydrologic parameters (e.g., porosity or hydraulic conductivity of the soil) (Livneh et al., 2015; Zacharias and Wessolek, 2007). In mHM, the soil moisture horizons/profile can be divided into several horizons, all of which are sensitive to root water uptake and evapotranspiration processes. mHM simulates the daily dynamics of soil moisture at different depths considering the incoming water (e.g., rainfall plus snow melt for the topmost layer and infiltration from above layers for other layers) and outgoing ET and ex-filtration fluxes. Further details on mHM code can be found at ~~https://mhm-ufz.org~~

155   https://mhm-ufz.org and underlying modelling concepts at Samaniego et al. (2010a); Kumar et al. (2013a).

2.3   Model Set-up

The latest version 5.12 of mHM is used in this study (see Samaniego et al., 2023, and https://github.com/mhm-ufz). The model is executed over six years (2014–2020) with a daily time step, and the spatial resolution of the mHM grid cells is fixed at ~~0.015625° (approx.~~ L1 and L2: 0.01562° x 0.01562° is eq.~ 1.2 ~~km ^{2})~~ km × 1.2 km using the WGS84 Coordinate

160   Systems. Level 1 (L1) describes the spatial resolution, as which dominant hydrological processes are modelled and Level 2 (L2) describes the resolution of the meteorological forcing data. L0: 0.001953125° × 0.001953125°. Level 0 (L0) describes the subgrid variability of relevant basin characteristics, which includes information on the soil as well as land use, topography, and geology.

Figure 2 shows the flow diagram depicting the basic methodology of our study, which includes the calculation of CRNS

165   neutron count rates ~~are calculated~~ based on daily soil moisture values simulated with mHM. The model boundary conditions such as precipitation and temperature for the mHM model are acquired from the German Weather Service (DWD) station closest to the test site. The potential evapotranspiration required by mHM is estimated using the Hargreaves-Samani method (Hargreaves and Samani, 1985). The model setup and parameterization for the soil moisture module use the scheme optimized by Boeing et al. (2022). A raster dataset describing the distribution of the soils in the model area and a corresponding lookup

170   table with the attributes depth, soil texture (sand and clay fraction), and bulk density are required as soil input data and are derived from national digital soil maps provided by the Federal Institute for Geosciences and Natural Resources (BGR, 2020). The data set contains physical and chemical properties for soil at different layers and the available at a resolution of 1:250,000 (BUEK 200; BGR, 2020). mHM uses three dominant land cover classes (forest, permeable, and impervious) that were retrieved by a GLOBCOVER database ESA (2009). Furthermore, vegetation characteristics like Leaf Area Index (LAI) and fraction of

175   roots for different vegetation types are prescribed in the model. The mHM soil domain is divided into three horizons with depths of 0–5 cm, 5–25 cm, and 25–60 cm. The upper two model layers are parameterized using the topsoil layer properties while for the lower model layer, the subsoil properties are used. More details on the underlying input data for mHM can be obtained from Boeing et al. (2022). ~~Figure 2 shows the flow diagram depicting the basic methodology of the entire study.~~
In our study, we utilized three distinct modules of parameters: Snow, Soil Moisture, and Neutrons, with a total of 29 parameters

180   employed for the Desilets method and 31 parameters for the COSMIC method. The simulation of soil water content is processed through these three modules to estimate neutron counts. To comprehensively cover the parameter set ranges, we employed 100 000 iterations. Finally, we selected the top 10 optimized parameter sets based on the objective function, $KGE_{\alpha\beta}$, for further analysis and evaluation.
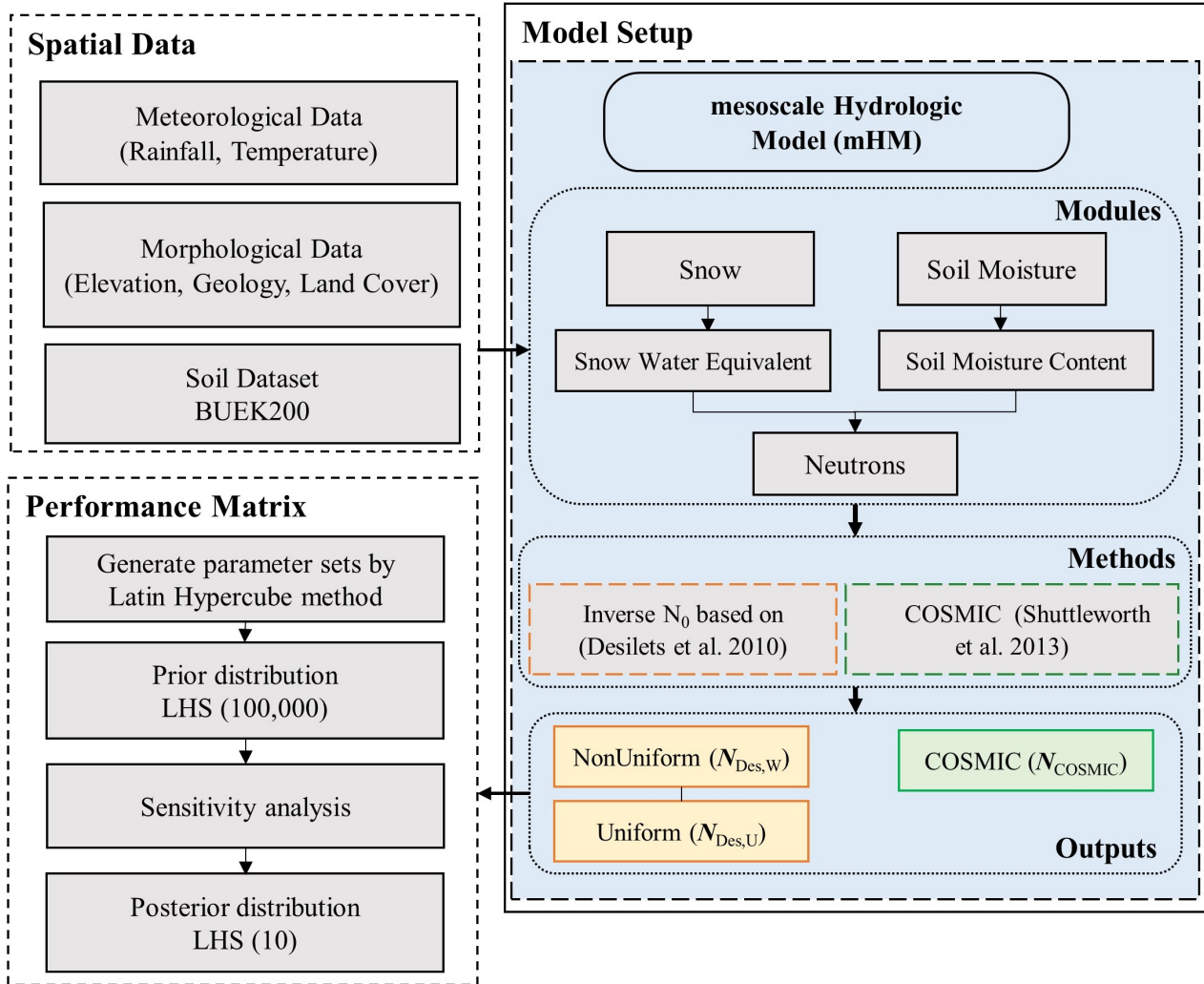
Figure 2. Flowchart depicting the methodology employed for calculating CRNS neutron counts through the utilization of the LHS technique for parameterization in mHM. The computation of CRNS neutron count is carried out through three distinct approaches: $N_{Des,U}$, $N_{Des,W}$, and N_{COSMIC}.

2.4 Conversion of soil moisture to neutron count rate

In this study, we compare observed neutron counts from CRNS data with simulated neutron counts estimated from modeled soil moisture with the goal of optimizing the parameterization of soil water content from mHM shown in Fig. 3. By coupling the approaches from Desilets et al. (2010) and Shuttleworth et al. (2013) each directly with the mHM model, we are able to account also for the uncertainty in the model predictions and test their feasibility across four distinct sites. We analyzed the soil water content data at different soil layers (0–5 cm, 5-25 cm, and 25-60 cm) ~~simulated by mHM. We compared these simulated values with the measured soil water content obtained through CRNS. Simulations from mHM revealed that the sensitivity to the highest soil water content was observed at 5 cm depth and decreased with increased depth, also indicating that SWC is high responsiveness to precipitation.~~ in mHM, as utilized in the study by Boeing et al. (2022). The accuracy of numerical calculations (such as Shuttleworth et al. (2013) set up) would benefit from higher resolved soil profiles, however, our experiments demonstrated that varying soil depths from 3 to 6 layers did not have a substantial impact on the simulated neutron count results in mHM. Our main objective is to optimize the parameterization of soil hydraulic properties in mHM based on the comparison between measurement and modelled neutron counts.
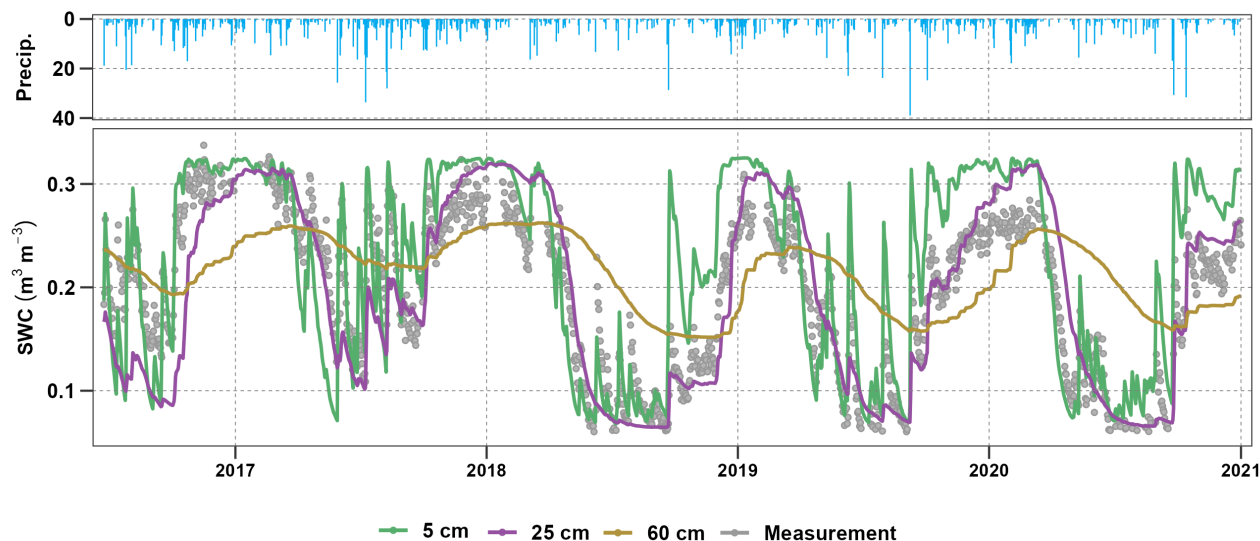
Figure 3. Daily time series of soil water content (cm^3cm^{-3}) at the *Cunnersdorf* site. The graph shows a comparison between the measured SWC from CRNS data representing an integral over the first decimeters and the simulated data derived from the mHM for three distinct soil depths, at 0–5 cm (green), 5–25 cm (purple), and 25–60 cm (brown).

2.4.1 Desilets based method

In the present study, we utilize the soil moisture information from the mHM model to convert it into neutron counts using the Desilets et al. (2010) empirical-based approach by calculating neutron counts from soil moisture, three constant parameters~~i.~~

~~e., a_0, a_1, a_2, and N_0,~~ which is further improved by adding lattice water and bulk density following the approaches by Dong et al. (2014) and Hawdon et al. (2014), respectively. Theoretically, the N_0 parameter, which represents the neutron count rate level of the particular CRNS probe used for rather dry soil at the local conditions, should be site-specific but does not change over time, as noted by Franz et al. (2013) and Hawdon et al. (2014). In order to obtain accurate measurements of soil moisture using CRNS data in the mHM model, N_0 has to be estimated through calibration and is crucial as it directly affects the accuracy of the mHM neutron counts results. This ~~time-constant~~ calibration parameter is specific to each site environment and reference condition. This parameter primarily depends on site-specific environmental factors and reference conditions. This coefficient is specific to the particular CRNS detector and may be impacted by factors such as ~~soil chemistry, vegetation cover, heterogeneity, and altitude~~ terrain (topography) but also local soil, vegetation characteristics, and additional hydrogen pools (e.g., from organic material) at each observation site Schrön et al. (2021). Therefore, calibration of N_0 is necessary for each CRNS data set at a site to ensure realistic model output. Neutrons are sensitive to all kinds of hydrogen in the footprint, hence the variable θ denotes not only soil moisture, θ_{sm}, but is rather assumed to also include lattice water, θ_{lw}, as well as water equivalent from soil organic carbon, θ_{org}, and vegetation biomass, θ_{bio}.

Soil moisture for three vertical mHM soil layers is used to drive both the Desilets method and the COSMIC operator. To improve comparability between measurements and modeling techniques, Schrön et al. (2017) propose the depth-weighted approach. This approach incorporates the contributions of different soil layers by calculating depth-weighted average SWC, θ_{avg}, resulting in a more comprehensive representation of soil moisture dynamics. This gives CRNS neutron count rates, after being corrected for incoming neutron flux, pressure, and air humidity variations, to be

$$N_{\text{Des}} = N_{0,\text{Des}} \left(\frac{a_0}{(\theta_{\text{avg}} + \theta_{\text{lw}})/(\varrho_b/\varrho_w) + a_2} + a_1 \right) \tag{1}$$

Among the four parameters, three of which are coefficients ~~(~~ parameters a_i were determined empirically by (Desilets et al., 2010) who derived $a_0 = 0.0808$, $a_1 = 0.372$, and $a_2 = 0.115$ ~~) derived from neutron particle physics modeling (Zreda et al., 2008; Desilets et al., 2~~, and are considered as constants for values of $\theta > 0.02\ gg^{-1}$. The fourth parameter, $N_{0,Des}$ is N_0 when using the Desilet's equation, and here is a free calibration parameter. Whereas the parameter θ_{lw} is the grid average volumetric water content of the equivalent lattice water content of the CRNS area ($\text{cm}^3\ \text{cm}^{-3}$), ϱ_b (g cm^{-3}) is the bulk density of the dry soil, usually determined from soil samples, and $\varrho_w = 1\ \text{g cm}^{-3}$ is the density of water. ~~Organic water equivalent (from~~ Regarding the variables of Soil Organic Carbon (SOC) and biomass ~~water equivalent,,~~ it's important to note that these variables are ~~frequently unknown, especially biomass~~ often not readily available, especially when it comes to biomass data. To address this, the free parameter N_0 is utilized to account for these unknowns. For lattice water, we assume a linear relationship to clay content (Avery et al., 2016):

$$\theta_{\text{lw}} = \theta_{\text{lw0}} \cdot \underline{C} \underline{C} \underline{C} + \theta_{\text{lw1}}, \tag{2}$$

~~CC~~ C denotes the clay fraction in % (Greacen, 1981). The derived quantity lattice water, θ_{lw}, is regionalized based on ~~CC~~ C and varies between 0.0 and 0.1 m^3/m^3. In order to obtain the average soil moisture for a layered soil moisture profile within mHM, the following averaging equation is employed:

$$\theta_{\mathrm{avg}}(w,\theta) = \frac{\sum_{i=1}^{n} w_i \theta_i}{\sum_{i=1}^{n} w_i} \tag{3}$$

where the volumetric soil water content at a specific layer of mHM in a given profile is denoted by θ_i (m^3 m^{-3}). The total number of layers in all soil sampling profiles is represented by the variable n, and the weight assigned to layer i is denoted by w_i. In the uniformly weighted approach, all weights equal one:

$$N_{\mathrm{Des,U}} = N_{\mathrm{Des}}(w_i = 1) \quad \forall\, i. \tag{4}$$

In the weighted-averaging approach, the weights are determined based on Schrön et al. (2017):

$$N_{\mathrm{Des,W}} = N_{\mathrm{Des}}(w_i = w\theta_{\mathrm{avg}}(z_i w, \theta)), \tag{5}$$

$$\text{where} \quad w(z)_i = \int_{z_{i,\mathrm{min}}}^{z_{i,\mathrm{max}}} e^{-2z/D - 2z/D}\, \mathrm{d}z \propto e^{-2\,z_{i,\mathrm{min}}/D} - e^{-2\,z_{i,\mathrm{max}}/D}$$

$$\text{and} \quad D = \varrho_b^{-1} \left(p_0 + p_1 \left(p_2 + e^{-p_3\, r} \right) \frac{p_4 + \theta}{p_5 + \theta} \right). \tag{6}$$

Here, the integral goes through each horizon from $z_{i,\mathrm{min}}$ to $z_{i,\mathrm{max}}$ in 1 mm steps and sums up the weight over the whole layer. z_i is the depth of the given soil moisture layer i, D is the average vertical footprint depth of the neutrons, p_i are numerical parameters presented in Schrön et al. (2017), and r (m) represents the distance from the sensor. It should be noted that the equation for ~~D seems to be valid only if bulk density does not get too small and SWC is not too high~~ D is valid for $\varrho_b > 1.0\,\mathrm{g\,cm^{-3}}$ and soil moisture contents above $\theta > 2\,\%$ Kasner et al. (2022). In our model, we set $r = 1$ m which is sufficient to represent the average depth across the footprint radius within the model grid. The soil moisture profile is converted to a single average neutron count per grid cell using Eqs. 1–5.

2.4.2 Cosmic Ray Soil Moisture Interaction Code (COSMIC)

The Cosmic Ray Soil Moisture Interaction Code (COSMIC) is an analytical, physics-based model that is well-suited for data assimilation applications. It includes descriptions of the degradation of incoming high-energy neutron flux with soil depth, the production of fast neutrons at each soil depth, and the scattering of resulting fast flux neutrons before reaching the soil surface. These processes have a parametric dependence on soil chemistry and moisture content. The COSMIC method solves this inverse problem by calculating ~~neutrons~~ neutron count rate based on soil water profiles, which could then be compared with observed neutrons without the need to deal with dynamic sensing depths or weightings.

$$N_{\text{COSMIC}} = N_{0,\text{COSMIC}} \sum A_{\text{high}}(z) X_{\text{eff}}(z) A_{\text{fast}}(z), \tag{7}$$

where $\quad A_{\text{high}}(z) = e^{-\Lambda_{\text{high}}(z)},$

$$A_{\text{fast}}(z) = \frac{2}{\pi} \int\limits_0^{\pi/2} e^{-\Lambda_{\text{fast}}(z)} (\cos\varphi)^{-1} \, d\varphi,$$

$$X_{\text{eff}}(z) = \alpha_{\text{COSMIC}} X_{\text{soil}} + X_{\text{water}}.$$

In this model, A_{high} represents the high-energy neutron attenuation, A_{fast} represents the fast neutron attenuation, and X_{eff} represents the production of fast neutrons from high-energy neutrons in the soil-water composite. It takes into account the different mechanisms in both, water and soil, where the soil is typically less effective in producing fast neutrons by a factor of $\alpha_{\text{COSMIC}} \approx 0.24$ (g cm^{3}g^{-1}), depending on bulk density.

$$X_{\text{soil}}(z) = \Delta z \varrho_{\text{b}}, \tag{8}$$

$$X_{\text{water}}(z) = \Delta z \varrho_{\text{water}}(\theta_z + \theta_{\text{lw}}), \tag{9}$$

The total attenuation lengths of high and fast neutrons in the ~~soil-water~~ soil water composite are described using physically motivated length scales L_i.

$$\Lambda_{\text{high}}(z) = \frac{X_{\text{soil}}(z)}{L_1} + \frac{X_{\text{water}}(z)}{L_2}, \tag{10}$$

$$\Lambda_{\text{fast}}(z) = \frac{X_{\text{soil}}(z)}{L_3} + \frac{X_{\text{water}}(z)}{L_4}. \tag{11}$$

The COSMIC function considers the attenuation of incoming high-energy neutrons (A_{high}) and their interaction with soil to produce effective neutrons (X_{eff}) in addition to the attenuation of isotropically propagating fast neutrons. The parameter α_{COSMIC} represents the soil's relative efficiency of forming fast neutrons, and length constants L_1, L_2, L_3, and L_4 (in ~~gcm^{-2}~~ g cm^{-2}) are related to local soil properties. COSMIC uses several time-invariant, site-independent, and site-specific parameters, including $L_1 = 162.0$ (g cm^{-2}), $L_2 = 129.1$ (g cm^{-2}), and $L_4 = 3.16$ (g cm^{-2}), as reported by Shuttleworth et al. (2013), regardless of location. However, the L_3 ~~parameters~~ (g cm^{-2}) ~~and α_{COSMIC} (g cm^{3}g^{-1})~~ parameter vary with soil bulk density ϱ_{b} which change with depth. ~~According~~ The parameter L_3 is correlated with the soil bulk density and according to the model code, L_{30} and L_{31} nomenclature are given as per the model code in mHM (https://github.com/mhm-ufz).

$$L_3 = L_{30}\varrho_{\text{b}} - L_{31}. \tag{12}$$

~~where θ_{lw0}, θ_{lw1} are the parameters of the lattice water and the equation of L_3 was taken from the dissertation of Schrön (2017)~~ The regional formulation of the COSMIC method has been revised to include the θ_{lw} lattice water content as well.

Besides the addition of lattice water to the code, the original version of COSMIC has also been numerically optimized to substantially increase the computational performance. This includes the calculation of the geometric integral (Eq. 7) based on lookup tables.

2.5 Constraining of model parameterization

In this study, we ~~utilize~~ employ a model calibration technique to identify the most suitable parameter values for the mHM

model. Specifically, we utilize a total of 29 parameters for the Desilets based method and 31 parameters for the COSMIC method which includes hydrologic processes related to: snow, soil moisture, and neutron counts dynamics. The process of model calibration involves modifying the parameter values of the model to achieve a satisfactory standard for an objective function by comparing the predicted output with the observed data (James, 1982). ~~In this study, we~~ We use the general concept of the ~~Kling-Gupta efficiency~~ KGE ~~for designing the objective function, which is widely employed in hydrological modeling to assess the efficiency of a model (Gupta et al., 2009). However, we modify the KGE~~ as a weighted combination of the three components (bias, variability, and correlation terms) to evaluate our simulation (Gupta et al., 2009). We excluded the correlation component from (Eq. 13) ~~by removing the correlation coefficient ρ, as it is just a measure of the temporal signature and is largely dominated by seasonality alone.~~ as our simulation already exhibited satisfactory correlation due to strong seasonality, we opted not to consider it in our assessment (objective function), as it accounted for 33% of the total weighting in the overall KGE score. Seasonality is an inherent characteristic in the northern hemisphere where precipitation minus evaporation is mostly driven by evapotranspiration. Even if a random parameter is selected correlation will always be higher because the meteorological forcing is the precipitation - evaporation is seasonal. This modified $KGE_{\alpha\beta}$ (Eq. 14) only depends on variability (α) and bias (β) and variants of it have been used also in other studies (see, e.g., Martinez and Gupta, 2010; Mai, 2023). We utilize observed neutron count data from CRNS and estimated neutron count data from the mHM model to calculate various metrics such as the Kling-Gupta efficiency coefficient ($KGE_{\alpha\beta}$), Nash-Sutcliffe efficiency (NSE) by Nash and Sutcliffe (1970), coefficient of determination (~~R^2~~R^2) by Kvålseth (1985), and percentage bias (PBIAS) by Gupta et al. (1999). The optimal PBIAS value is 0, with lower values indicating more accurate model simulations. Positive values indicate underestimation by the model, while negative values indicate overestimation. This approach allows us to minimize uncertainty in the simulated neutron count data by comparing it to observed data and determining the optimal parameter values for the mHM model. A summary of the individual parameters and their ranges can be found in ~~Table~~Supplementary Table S1 and

model performance measures are shown in Table 2.

$$KGE = 1 - \sqrt{(\alpha - 1)^2 + (\beta - 1)^2 + (\rho - 1)^2}, \tag{13}$$

$$KGE_{\alpha\beta} = 1 - \sqrt{(\alpha - 1)^2 + (\beta - 1)^2}, \tag{14}$$

with Variability $\alpha = \sigma_{\text{sim}}/\sigma_{\text{obs}}$, $\qquad\qquad\qquad\qquad\qquad\qquad\qquad\qquad\qquad\qquad\qquad\qquad\qquad\qquad$ (15)

Bias $\beta = \mu_{\text{sim}}/\mu_{\text{obs}}$, $\qquad\qquad\qquad\qquad\qquad\qquad\qquad\qquad\qquad\qquad\qquad\qquad\qquad\qquad$ (16)

Correlation $\rho = \rho(\text{sim}, \text{obs})$,

$$NSE = 1 - \frac{\sum_{i=1}^{n}(y_{\text{sim,i}} - y_{\text{obs,i}})^2}{\sum_{i=1}^{n}((y_{\text{obs,i}} - \overline{y}_{\text{obs,i}})^2}, \tag{17}$$

$$R^2 = \left(\frac{\sum_{i=1}^{n}(y_{\text{obs,i}} - \overline{y}_{\text{obs,i}})(y_{\text{sim,i}} - \overline{y}_{\text{sim,i}})}{\sum_{i=1}^{n}\sqrt{(y_{\text{obs,i}} - \overline{y}_{\text{obs,i}})^2}\sqrt{(y_{\text{sim,i}} - \overline{y}_{\text{sim,i}})^2}} \right)^2, \tag{18}$$

$$PBIAS = 100[\%](1 - \beta). \tag{19}$$

Table 2. Performance evaluations for the daily neutron counts simulation with observed CRNS dataset.

Indices	$KGE_{\alpha\beta}$	KGE	NSE	R^2	PBIAS
Range	$-\infty$ to 1	$-\infty$ to 1	$-\infty$ to 1	0 to 1	$-\infty$ to ∞
Optimal Value	1	1	1	1	0
Satisfactory Value	> 0.70	> 0.80	> 0.50	> 0.65	$< \pm 5$

3 Results

3.1 Constraining of the parameter distribution ~~N0~~ N_0 / Sensitivity Analysis

The sensitivity and uncertainty analysis performed in this study use a Latin Hypercube Sampling (LHS) approach, resulting in parameter distributions that ~~almost cover the entire prior defined hypercube of the individual parameters.~~ large sample size was chosen to comprehensively explore the parameter sets and capture a wide range of possible parameter combinations in the prior range. The LHS approach creates a random value between the min and max values of the parameter set. Initial parameter ranges and exploratory model runs are set based on literature values (Boeing et al., 2022; Kumar et al., 2013b). Supplementary Table S1 shows the values for the parameters in all ~~10~~100 000 simulations and the selected 29 parameters for the Desilets method and 31 parameters for the COSMIC method, which include snow, soil moisture, and neutrons modules as behavioral simulations, with the posterior mean of the top 10 best parameters set. For further information and additional details about the calibrated parameters for each site, refer to Supplementary Table S2. Among the calibrated parameters, the N_0 parameters are different in each method since this parameter ~~has not exactly~~ does not exactly have the same physical meaning in the Desilets and the ~~COSMOS models~~COSMIC methods.

~~In~~

Fig. 4 ~~the *x*-axis in each graph is fixed to the prior range of each individual parameter to facilitate the comparison of sensitive parameters. Most of the high-sensitive parameters show more peaked densities in a narrower range of parameter values, reflecting the significance of variations in model parameter values~~ displays the x-axis in gray, representing the original parameter range (600–1500) prior distribution for the Desilets method and (100–400) for COSMIC method. Meanwhile, the colored sections in brown, green, and purple indicate the parameter values of the calibration from the posterior distribution taken from the top-performing parameter sets for each study site. The most sensitive parameters during the calibration period are $N_{0,\text{Des}}$, $N_{0,\text{COSMIC}}$, rootFractionCoefficient_pervious, and rootFractionCoefficient_forest of land cover classes are employed: class 1 = forest which consisted of permeable areas covered by coniferous, deciduous, and mixed forests; class 2 = impervious cover with land uses like settlements, industrial parks, roads, airport runways, and railway tracks; and class 3 = permeable cover covered by fallow lands, or those surfaces covered by crops, grass, and orchards. The calibration process notably ~~sharpenes~~ sharpens the Probability Density Function (PDF) of these significant parameters by eliminating some of the uncertainty linked to the variance in the prior probability distributions.

~~The uniform prior distribution range for $N_{0,\text{Des}}$ lies between 600 and 1500 cph, and $N_{0,\text{COSMIC}}$ lies between 100 and 400 cph.~~ For agricultural sites such as *Cunnersdorf* and *Hordorf*, the $N_{0,\text{Des}}$ best estimate parameter results lie between 1000 and 1400 cph. Meanwhile, for *Hohes Holz*, the $N_{0,\text{Des}}$ parameter range lies between 800 and 1000 cph, the lowest value for the calibration parameter $N_{0,\text{Des}}$ is found between 800 and 900 cph due to the highest wet above biomass in the forest area. Similarly, for *Grosses Bruch* sites, the lowest value for the calibration parameter $N_{0,\text{Des}}$ is found between 800 and 900. The prior parameter distribution $N_{0,\text{Des}}$ 600 and 1500 cph is the same for all four experiments.

The estimated values of $N_{0,\text{Des}}$ and $N_{0,\text{COSMIC}}$ obtained in our study are close to the optimal values, indicating that the model has the potential to generate accurate cosmic-ray soil moisture estimates even under dry conditions. ~~But since at least COSMIC is physically based, a loss of the physical meaning of the parameters in question would be very critical.~~ In contrast, some hydrological models, such as HBV and PREVAH (PREecipitation Runof EVApotranspiration Hydrological response unit model; Viviroli et al. 2009), have demonstrated weaker performance in simulating soil moisture, particularly during dry conditions (Orth et al., 2015), with slightly better agreement with observations observed during wet conditions. Table 3 provides detailed information on the mean and 95% confidence interval (CI) of the parameter values of the prior and posterior simulated results of N_0. One of the important addition of this work is incorporating the lattice water account and we used the regionalization equation to calculate the lattice water which depends on the clay content with free parameters in Eqs. 2. The optimized parameter of the mHM shows the variation of the θ_{lw} ranges between (0.02–0.04) cm^{3}cm^{-3} for different sites (see Supporting Information Table S3). This behaviour and the way it was defined in Eq. 1 indicate that θ_{lw} likely represents not only soil lattice water itself, but rather the total offset of all hydrogen pools in the vicinity of the sensor (see e.g., Schrön et al., 2017; Iwema et al., 2021).
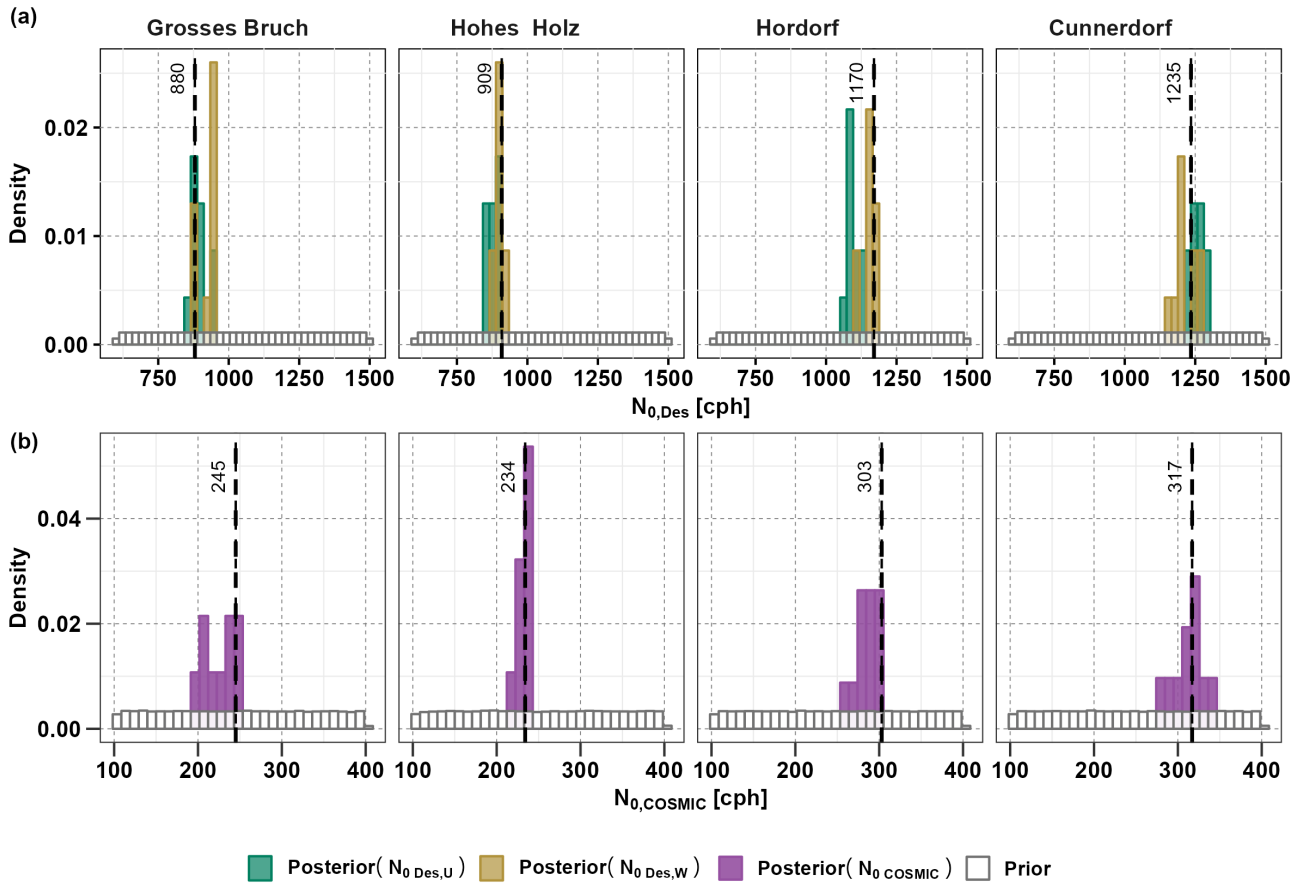
Figure 4. Probability Density Function (PDF) of the mHM parameter N_0 [cph] for two different approaches: (a) the Desilets method, and (b) the COSMIC method. The prior PDF of the original sample, consisting of 100 000 data points, is represented by the grey color. The behavioral PDF, obtained after applying the objective function, is shown for weighted (~~orange~~brown), uniform (green), and COSMIC (purple). The black dashed line represents the one N_0 [cph] value that best fits the data.

Table 3. The four most right columns are the posterior ones of size 100 000 and are the same for all sites. The posterior distributions correspond to the distributions in the behavioral sample obtained after the application of the objective function. The values correspond to the median (Q_{50}) and the lower and upper bound of the 95% confidence interval ($Q_{2.5}$ and $Q_{97.5}$, respectively).

Parameter	CI	Prior	*Grosses Bruch*	*Hohes Holz*	*Hordorf*	*Cunnersd...*
$N_{0(\text{Des,U})}$	Q_{50}	1050	889	882	1092	
	$Q_{2.5}$	623	866	855	1069	
	$Q_{97.5}$	1477	945	908	1126	
	mean	1050	899	883	1096	
	sd	260	27	21	21	
$N_{0(\text{Des,W})}$	Q_{50}	1050	942	906	1158	
	$Q_{2.5}$	623	876	871	1116	
	$Q_{97.5}$	1477	954	915	1176	
	mean	1050	925	899	1152	
	sd	260	34	16	21	
$N_{0(\text{COSMIC})}$	Q_{50}	250	225	234	287	
	$Q_{2.5}$	108	202	216	265	
	$Q_{97.5}$	392	249	241	302	
	mean	250	226	232	285	
	sd	87	18	9	12	

3.2 Time series analysis of simulated neutron counts

The study conducts simulations of neutron counts in mHM using soil moisture parameterizations, with results presented in Figs. 5–6 across different sites. The simulated neutron counts were based on the simulated soil moisture content at the modeled soil horizons i.e., 0–5 cm, 5–25 cm, and 25–60 cm. The results of the ensemble runs show that the precision is higher for the behavioral simulation ensembles 0.1 % (represented by dark gray shaded areas) than in the unconstrained simulated data 1 % (represented by light gray shaded areas). We select the best 0.1 % with the highest KGE from 100 000 model runs, and the results are presented in Tab. 4. ~~Furthermore, the behavioral simulation ensembles captured more variations in the COSMIC method compared to the Desilets method after the application of the objective function (i.e., KGE$_{\alpha\beta}$).~~

The N_{COSMIC} method performs best at the forest site (*Hohes Holz*), whereas at the agricultural sites (*Hordorf* and Cunnerdorf), the $N_{\text{Des,W}}$ method performs slightly better. Only for the grassland site (*Grosses Bruch*), the uniform method $N_{\text{Des,U}}$ slightly outperforms the other two methods i.e., $N_{\text{Des,W}}$ and N_{COSMIC}, while overestimating the observations at all the other sites. ~~The better performance of N_{COSMIC} and $N_{\text{Des,W}}$ over $N_{\text{Des,U}}$ demonstrates the benefits of explicitly resolving individual soil moisture profiles, bulk densities, and lattice water, as opposed to a uniform average across the layers. This perception, however, might depend on site-specific soil profile characteristics and be less prominent if profiles are largely uniform or~~

~~incorrectly resembled by the model structure.~~ In general, we observe good model performance for all methods indicated by a correlation coefficient greater than 0.80 and a percent bias (PBIAS) below 2 % across the majority of investigated sites and methods.

These results suggest that the neutron-forward models match the observed neutron counts well. However, the mean ensemble had difficulties reproducing the neutron counts for the *Grosses Bruch* site in all three methods. ~~One of the primary sources of uncertainty at the *Grosses Bruch* site is surface ponding and shallow groundwater, as well as the loamy texture of the soil. Those factors contribute to the formation of permanent water ponds in the area and may introduce uniform or even inverse soil moisture profiles which directly influence the neutron emissions, but cannot be captured by the mHM model. Another factor is the time-variable effect of crowding cows near the station, which may influence the CRNS signal, but is challenging to correct in the CRNS measurement (Schrön et al., 2017).~~

~~We incorporate the CRNS parameter set in mHM, and some parameters related to soil moisture and neutron counts are effectively constrained based on the objective function using KGE$_{\alpha\beta}$. However, there is still room for improvement, particularly with regard to the coefficient in root fractions distributed across soil layers.~~ The incorporation of dynamic vegetation in models is important as it can impact the model parameter LAI, which in turn can affect root water uptake and soil water content. Currently, these factors are not considered in the models, leading to a permanent and systematic shift in these variables each year (Zink et al., 2017; Massoud et al., 2019).

The results also highlight the uncertainties associated with model simulations and the sensitivity of the objective function. We find that three soil moisture-related parameters, namely N_0, *rotfrcoffpre*, and *rotfrcofforest*, have the most significant impact on the objective function KGE$_{\alpha\beta}$, compared to the other parameters of mHM. The parameter N_0 directly affects the neutron count simulations, while the parameters *rotfrcoffpre* and *rotfrcofforest* correspond to the fractions of vegetation roots in different soil layers that directly affect the water availability related stress for the estimation of actual evapotranspiration, and thereby the soil-water dynamics (Samaniego et al., 2010b; Kumar et al., 2013b). The best parameter set values in mHM across all sites and methods are given in (Supporting Information Table S2).
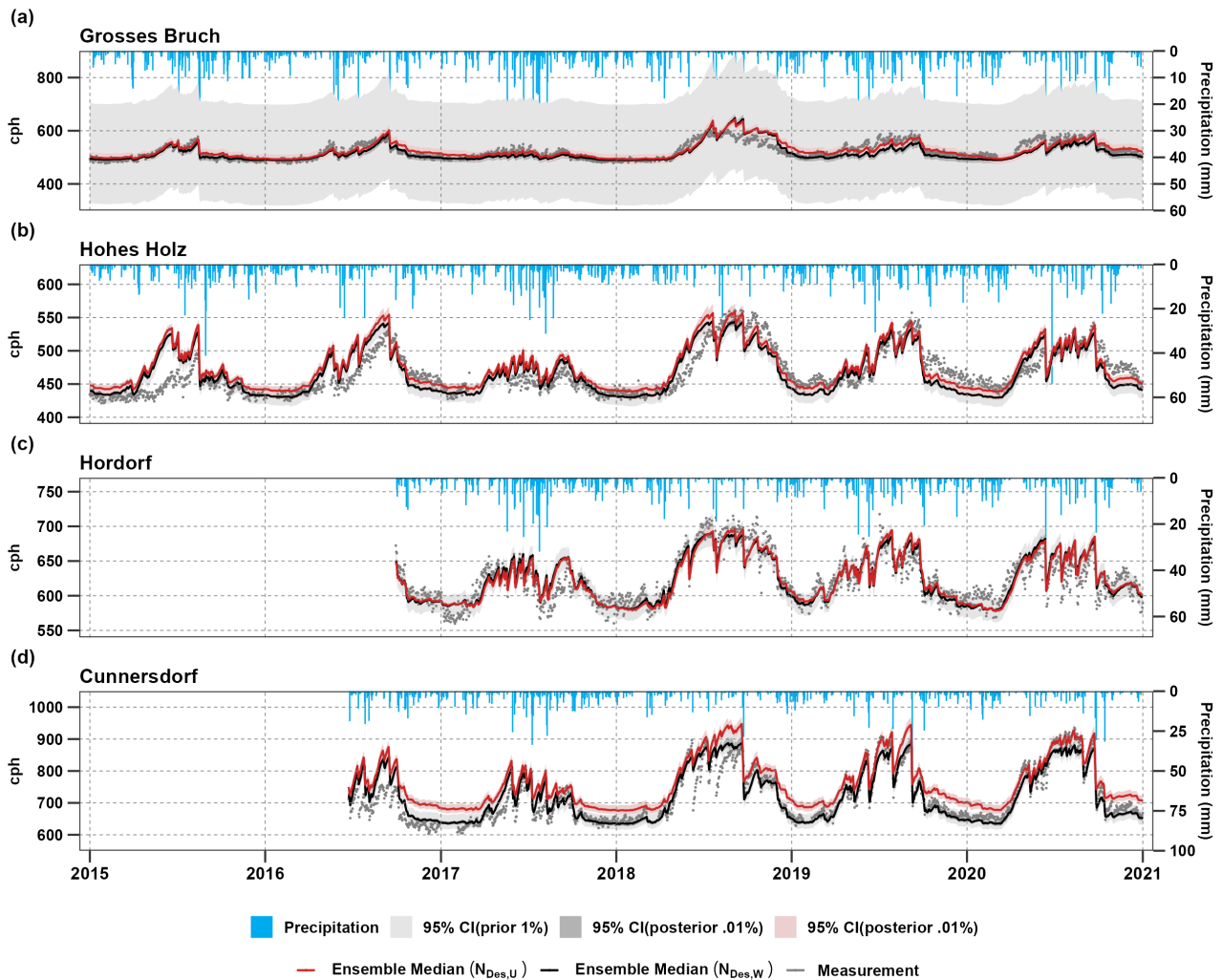
Figure 5. Simulated daily time series of black for ~~N(Des,W)~~ $N_{Des,W}$, red for ~~Nsim(Des,Uni)~~ $N_{Des,U}$ for the four sites. The black lines represent the median of the behavioural simulation ensembles that satisfy the objective function which is LHS10 ensemble members. The light grey shaded areas represent the 95% CI of the simulation ensembles corresponding to different levels of constraining which is LHS1000 ensemble members, and the observation is shown in grey points. Precipitation is shown in blue color on the top.
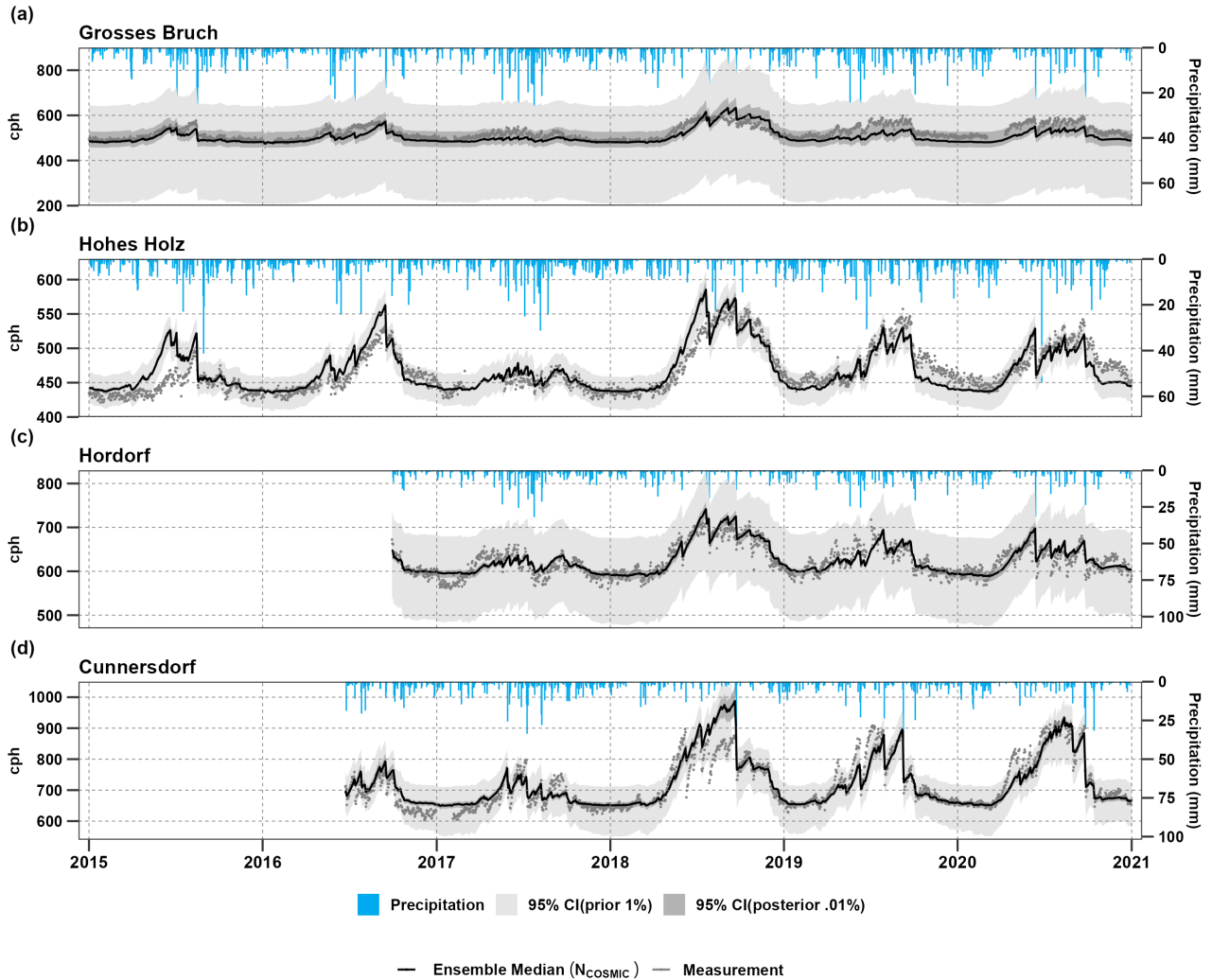
Figure 6. Simulated daily time series of ~~N(COSMIC)~~ N_{COSMIC} for the four sites. The black lines represent the median of the behavioural simulation ensembles that satisfy the objective function which is LHS10 ensemble members. The light grey shaded areas represent the 95% CI of the simulation ensembles corresponding to different levels of constraining which is LHS1000 ensemble members, and the observation is shown in grey points.

3.3 Model calibration statistics and evaluation

In addition to KGE$_{\alpha\beta}$, the four metrics KGE, NSE, R, and PBIAS are used to evaluate further the mHM neutron counts simulated with observed CRNS data. We employ LHS to generate a parameter sample of 100 000 for the three methods, namely $N_{Des,U}$, $N_{Des,W}$ and N_{COSMIC}, by uniformly distributing the ranges provided in the (supplementary Table S1). The top 10 parameter sets are found to perform satisfactorily with a KGE range of 0.80 to 0.93, as demonstrated in Table 4. The

calibrated parameter sets obtained from different objective functions are also evaluated and compared using various statistical indices, as shown in Figure 7, with most objective functions performing better than satisfactory based on the criteria in Table 2. The results for the COSMIC method indicate that the main contribution to poorer results during the evaluation period was due to the variability term (α). The boxplot displayed in Figure 7 illustrates the threshold achieved by the top 1000, 100, and 10 LHS members, along with the corresponding percentage of the best 10 LHS parameter sets that meet the threshold, as specified in (see Tab. 2). Among the 31 parameters selected to simulate neutron counts, this plot provides an overview of the distribution of results and their variability with respect to the threshold criteria.

Table 4. ~~Model~~ Performance metrics for model calibration (2014-2021) using various methods: Percent bias (~~Pbias~~PBIAS), coefficient of determination (R^2 R^2), Nash-Sutcliffe efficiency (NSE), and Kling-Gupta Efficiency (KGE) ~~for~~ across different sites. Bold values indicate the ~~calibration for the period from 2014-2021~~best performance measures.

Sites	Grosses Bruch			Hohes Holz			Hordorf			Cunnersdorf		
Methods:	$N_{\text{Des,U}}$	$N_{\text{Des,W}}$	N_{COSMIC}	$N_{\text{Des,U}}$	$N_{\text{Des,W}}$	N_{COSMIC}	$N_{\text{Des,U}}$	$N_{\text{Des,W}}$	N_{COSMIC}	$N_{\text{Des,U}}$	$N_{\text{Des,W}}$	N_{COSMIC}
$\text{KGE}_{\alpha\beta}$	**0.97**	0.96	0.93	0.96	**0.99**	**0.99**	**0.99**	**0.99**	0.98	0.93	**0.99**	**0.99**
KGE	**0.85**	0.83	0.81	0.81	0.80	**0.85**	**0.87**	**0.87**	0.86	0.88	**0.93**	0.90
NSE	**0.69**	0.60	0.29	0.54	0.60	**0.70**	**0.75**	**0.75**	0.73	0.57	**0.85**	0.79
R^2	**0.73**	0.69	0.66	0.66	0.65	**0.73**	**0.76**	**0.76**	0.75	**0.86**	**0.86**	0.81
R	**0.85**	0.83	0.81	0.81	0.80	**0.85**	**0.87**	**0.87**	0.86	**0.93**	**0.93**	0.90
PBIAS	**0.7%**	-1.3%	-3.3%	2.0%	**0.3%**	0.4%	**0.1%**	**0.1%**	0.3%	6.0%	0.7%	**0.5%**
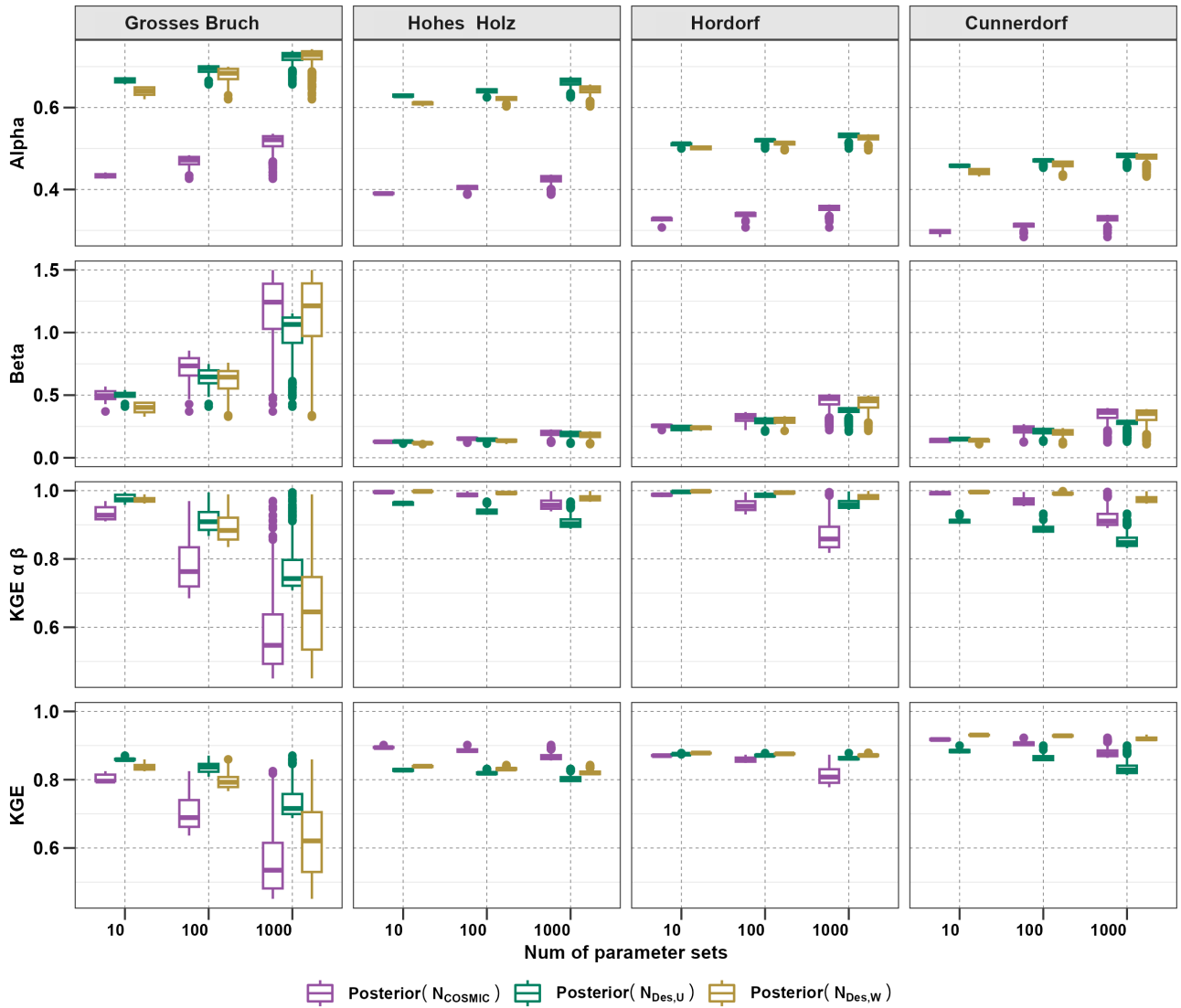
Figure 7. Evaluation of model performance using boxplots constraining of 1000 to the best 10 parameters set at four different sites, using three different methods, namely ~~N(Des,W)~~ $N_{Des,W}$ in ~~red~~brown, ~~N(Des,Uni)~~ $N_{Des,U}$ in ~~golden~~green, and ~~N(COSMIC)~~ N_{COSMIC} in purple. The figure presents four subplots, where (a) represents Alpha, (b) Beta, (c) ~~KGEαβ~~$KGE_{\alpha\beta}$, and (d) Kling-Gupta efficiency (KGE) and its components, i.e., the variability term (perfect value: 1), and bias term (perfect value: 1), respectively.

3.4 ~~Evapotranspiration evaluation~~ Comparing evapotranspiration at Hohes-Holz: eddy covariance ~~stations~~ observed data ~~against~~ vs mHM simulation

The ensemble model of (10 members) simulations, is further examined with the evapotranspiration (ETa) to cross-evaluate and assess the model's ability to represent other fluxes and states next to neutron counts by using the ETa observational data

from eddy covariance measurements Integrated Carbon Observation System (ICOS) at *Hohes Holz* Warm Winter (2022). In terms of temporal dynamics, the model is able to capture the observed ETa quite well at the study site, as shown in Figure 8.

415   Panel (c) displays the scatter plot ~~that reveals no systematic over or underestimation of the observed actual evapotranspiration. The~~ incorporating linear regression models to quantify the relationships between observed and mHM-simulated ETa during both the growing and non-growing seasons. This plot provides insights into the seasonal variations in the relationship between observed and simulated ET. It suggests that the model performs best during winter, while its performance during summer is comparatively weaker. The correlation coefficients (r values) for each season are as follows: autumn [SON] (r = 0.79),

420   spring [MAM] (r = 0.77), summer [JJA] (r = 0.42), and winter [DJF] (r = 0.87). It is worth noting that winter shows the highest correlation between observed and simulated ET, while summer exhibits the lowest correlation. The most significant deviation in terms of RMSE is evident during the summer, when evapotranspiration is highest, while the smallest difference is in winter when evapotranspiration has less impact. The model slightly overestimates evapotranspiration in summer and spring, possibly because of the absence of a dynamic vegetation growth module in the mHM, also discussed for evapotranspiration in

425   Zink et al. (2017). The temporal dynamics of the model-simulated evapotranspiration are in good agreement with the observed data from the *Hohes Holz* forest eddy covariance site, taken from Warm Winter (2022), as illustrated in Figure 8a. The daily correlation between observed and simulated evapotranspiration is observed high in the growing season at $r = 0.84$, whereas the lowest correlation is found in the non-growing season at $r = 0.65$ in Figure 8c. The highest deviation in terms of RMSE is observed during summer when the highest fluxes occur, and the lowest during winter, in which the contribution of ETa is

430   lowest.

In Figure 8b, the prior and posterior parameter distributions of evapotranspiration for *Hohes Holz* are displayed. The prior distribution represents the ~~10~~100 000 parameters set utilized for the neutron counts simulation under Latin Hypercube Sampling (LHS). The results demonstrate that the ensemble model of 10-member simulations (posterior) for neutron counts can also effectively capture evapotranspiration, exhibiting a root mean square error (RMSE) of 0.76 mmd^{-1} of the growing season and

435   0.25 mmd^{-1} for non-growing when compared to observed ICOS data and simulated mHM. When compared to the model simulations with ~~a priori~~ prior parameter sets, we notice a substantial improvement in ET simulations (mean RMSE of 0.86 mmd^{-1} to 0.76 mmd^{-1}). Furthermore, the RMSE range is also narrower for the posterior simulations compared to the prior ones which further demonstrated the additional value of incorporating CRNS measurements in improving the consistency of both modeled soil moisture and evapotranspiration estimates.

440   ~~The modeled evapotranspiration is highly dependent on soil parameterization because soil water is the main source of evaporative water. During the growing season (summer), the model exhibited the largest variability in modeled ETa (Figure 8c). This can be associated among other things with a lack of a dynamic vegetation growth module in mHM, which may not capture the onset of the vegetation period adequately. This variability could also be attributed to seasonal changes in vapor pressure difference (VPD) or more localized processes occurring at the forest site (e.g., under-story vegetation), which are currently not~~

445   ~~considered in the model.~~ Nevertheless, the overall agreement between modeled and observed ETa is reasonably good; and the analysis reveals further improvement of model performance in the growing season.
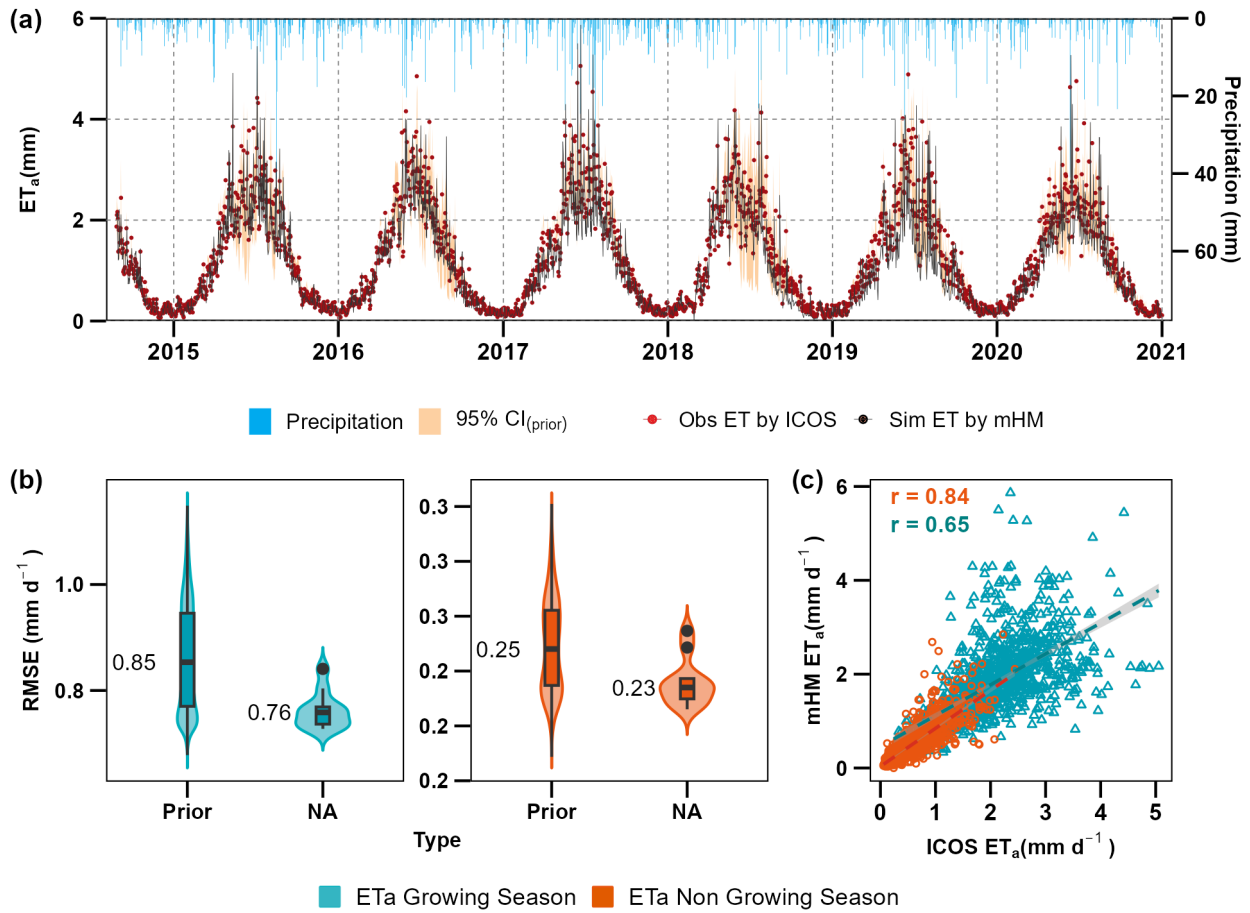
Figure 8. (a) Time series of actual evapotranspiration (ETa) from mHM (black), ICOS measurement (red), and the prior range of 100 000 realizations in (orange) color. (b) Boxplot of daily actual evapotranspiration (ETa) differences between the growing and non-growing seasons, comparing two selected prior with ~~10~~100 000 simulations, the values represent the mean of the statistical metrics and posterior with 10 ensemble member distributions using the root mean square error (RMSE) as the evaluation metric (μgm^3). (c) scatterplots of modeled vs. observed ET on a daily basis from ICOS during the growing season from March to August (green) and non-growing season from September to February (brown) at *Hohes Holz* eddy covariance station in a forest.

4 Discussion

This study assessed the suitability of CRNS observations at four sites to enhance soil moisture representation in mHM. ~~The model's depth-dependent simulations allow the estimation of neutron penetration depths, which are typically 5–60 cm and more sensitive to shallow soil moisture Köhli et al. (2015). Our findings contribute to leveraging CRNS data for improved~~

hydrological modeling. ~~The theoretical measurement depth for the cosmic-ray probe varies, ranging from $\sim$ 12 cm in wet soils to $\sim$ 76 cm in dry soils (Zreda et al. (2008, 2012a); Rosolem et al. (2014)).~~

To improve the soil moisture profile representation within mHM it is a major challenge to use a single vertically integrated CRNS measurement. In order to have a fair comparison between the model and observed CRNS data, two conceptually different approaches were integrated into mHM to calculate neutron counts from different SWC horizon depths i.e., an empirical method based on Desilets et al. (2010), and a physics-based method (COSMIC) based on Shuttleworth et al. (2013). Since the empirical method is described by an analytical expression, taking into account the uniform average of the soil moisture layers, it is straightforward to implement and therefore most commonly used (Zreda et al., 2012b; Rivera Villarreyes et al., 2011; Andreasen et al., 2017; Bogena et al., 2022). However, the method comes with the risk of missing a representation of the vertical profile of soil properties and water content. Therefore, we extended this uniform-averaging scheme ~~by~~ with a vertical weighting scheme to mimic the sensitivity of the neutrons to the upper layers both weighted and non-weighted soil moisture approaches in the context of CRNS have been discussed (Rivera Villarreyes et al., 2014; Baroni and Oswald, 2015; Schreiner-McGraw et al., 2016; Zreda . The COSMIC operator also accounts for the full soil moisture profile, but in a more physically behaved manner, following the track and attenuation of the neutrons in and out of the soil column. The mHM model is now able to simulate neutrons directly with all three approaches. The presented results confirmed general consistency with CRNS observations at four sites in Germany (Figs. 5 and 6).

Agricultural land presents a valuable opportunity to examine the interaction between soil moisture dynamics, crop growth, irrigation methods, and vegetation dynamics. *Hordorf* and ~~Cunnerdorf~~ *Cunnerdorf* are specific agricultural sites where seasonal changes in aboveground biomass are expected to be larger due to crop growth and harvest compared to grassland and forest sites. The study by Schrön et al. (2017) found that the revised weighting strategy for CRNS data improved the accuracy of soil moisture predictions at agriculture sites, but there is still room for improvement in capturing local dynamics through revised parameters in the CRNS model. Our results showed that at the agriculture site, the ~~$N_{0,\text{Des,w}}$~~ $N_{\text{Des,w}}$ methods in mHM slightly out-performed the other methods.

We also investigated *Hohes Holz*, a forest site, and observed an early simulation of approximately 28 days in the simulation of neutron counts compared to the observations. The early simulation phase could be attributed to the limitation of mHM in simulating the dynamics of detailed vegetation mechanisms Zink et al. (2017). One specific limitation is that the model does not fully account for the fact that trees at the site have access to deeper water sources, which can result in water stress being experienced at later times. Still, we get very good results in terms of KGE, for instance, indicating that these issues are of minor importance and that all three methods in mHM representation of the forest are already performing quite well. ~~Also, the CRNS method may be influenced by temporal biomass variation in the forest (Baatz et al., 2015), but many recent studies have confirmed the good performance of CRNS in forests compared to below-ground soil moisture profiles, indicating that the dynamic vegetation effect is just a minor observational issue (Bogena et al., 2013; Andreasen et al., 2017; Schrön et al., 2017; Boeing et al., 2022; Bogena et al., 2022 . It is worth noting that most of the studies on drought analysis look at the anomaly of soil moisture, while our study tries to assess the absolute soil water quantity and the properties that can determine the soil water content.~~ While CRNS and TDR generally agree at this site, the discrepancy shown in our results could be attributed to issues related to process representation in

mHM Boeing et al. (2022). Simulation of neutron data within the mHM model and subsequently comparing it with observed counts can enhance the accuracy and precision of soil moisture measurements. Future research can focus on exploring the potential relationships between CRNS data and soil moisture anomalies, thus furthering our understanding of the dynamics of drought and assisting in the development of efficient drought monitoring and mitigation strategies.

To cross-evaluate our results, we generated and filtered the 100 000 regionalized parameter sets based on observed neutron counts for behavioral solutions. After selecting the most effective solutions, we conduct cross-validation by comparing the mHM simulations of evapotranspiration against observational data from eddy covariance measurements ICOS (Warm Winter, 2022; Pohl et al., 2023) at the *Hohes Holz*. Figure 8 shows the scatter including the seasonal correlation coefficient at the forest site. The results indicate low correlations in summer, likely due to mHM's limitations in capturing evapotranspiration values with mHM's static vegetation module. However, the model performs well in winter, with a high correlation between observed and simulated values of evapotranspiration, the results confirm the findings from Zink et al. (2017), who used mHM to estimate evapotranspiration, groundwater recharge, soil moisture, and runoff with 4 km spatial and daily temporal resolutions (1951–2010). They utilized soil moisture observations from eddy covariance stations employing Time-Domain Reflectometer (TDR) or Frequency-Domain Reflectometer (FDR) sensors. Due to disparities in spatial representativeness and sampling depth, a direct comparison between observed and simulated soil moisture was not feasible, their findings revealed deviations in evapotranspiration during spring and in cropland areas, while soil moisture estimations exhibited good agreement with observed dynamics. The study highlights the importance of considering seasonal variations when analyzing the results. Discrepancies, such as low correlations in summer, indicate the need for improvements in capturing evapotranspiration dynamics under varying environmental conditions. Refining vegetation dynamics representation could enhance the simulation of evapotranspiration processes. Additionally, the agreement between mHM and observed soil moisture dynamics suggests variable model performance for different hydrological variables, emphasizing the need for a comprehensive assessment of its capabilities across various environmental conditions and spatiotemporal scales.

The accuracy of modeled evapotranspiration is linked to soil parameterization because soil water is the main source of evaporative water. During the growing season (summer), the model exhibited the largest variability in modeled ETa (Figure 8c). This can be associated among other things with a lack of a dynamic vegetation growth module in mHM, which may not capture the onset of the vegetation period adequately. This variability could also be attributed to seasonal changes in vapor pressure difference (VPD) or more localized processes occurring at the forest site (e.g., under-story vegetation), which are currently not considered in the model. The comparison of observed neutron counts with simulated counts from mHM improved not only soil moisture estimation but also evapotranspiration estimation in the model. This provides evidence that CRNS data has the potential to improve hydrological process understanding as a whole.

The *Grosses Bruch* site stands out as a mesophilic grassland site with a nearby water channel, shallow ground water, regular cattle grazing, and seasonal flooding (Hermanns et al., 2021). We find a large ensemble-related uncertainty at this site for all

three methods, while the uniformly weighted approach $N_{\text{Des,U}}$ shows a slightly better performance than the other two methods $N_{\text{Des,W}}$ and N_{COSMIC} (see Table. 4). The behaviour may result in a missing representation of locally significant hydrological components, such as dynamic biomass, snow, shallow ground water, or nearby surface ponding (Schrön et al., 2017). Moreover, in the middle of September, many cows had been present at this site, which could have led to a non-negligible variation of the neutron signal and thus to a non-meaningful expression of correlation-related measures Schrön et al. (2017). Döpper et al. (2022) mentioned thigh impact of grazing on the plant traits and soil properties at this site. Additionally, the use of one grid cell measurements by mHM in our study may have limited the accuracy of our results, as the depth of measurement may not be representative of the entire soil profile. Notably, neutron counts were found to provide a more accurate representation of soil water content during June, July, August, and September, when levels tend to be lower. Further exploration of neutron counts may yield additional improvements to model performance.

Overall, the three methods ($N_{\text{Des,U}}$, $N_{\text{Des,W}}$, and N_{COSMIC}) in mHM were able to consistently simulate the neutron count variability throughout the available data period. However, a broader confidence interval is observed, indicating a greater range of variations, which implies a higher degree of uncertainty in the N_{COSMIC}. The COSMIC approach explicitly accounts for water content snow, vegetation interception, and root-zone soil processes that may likely lead to a better representation of observed neutron count variation compared to Desilets that empirically represent such processes. The simulated time series tended to slightly underestimate the CRNS neutron count rate, particularly during the dry season. This effect could be explained by the known limitations of the equations under very dry conditions, while recent approaches exist (Köhli et al., 2021) that could lead to further improvement in future studies. Nevertheless, the results generally confirmed the better performance of the $N_{\text{Des,W}}$ than $N_{\text{Des,U}}$, because of its more realistic representation of neutron propagation with depth. After optimizing the soil hydraulic properties based on CRNS data, the integrated signal was reproduced very well (Fig. 5). The better performance of N_{COSMIC} and $N_{\text{Des,W}}$ over $N_{\text{Des,U}}$ demonstrates the benefits of explicitly resolving individual soil moisture profiles, bulk densities, and lattice water, as opposed to a uniform average across the layers. This perception, however, might depend on site-specific soil profile characteristics and be less prominent if profiles are largely uniform or incorrectly resembled by the model structure. We also included offset hydrogen pools in the form of lattice water to the N_0 calibration function, which was important for more accurate soil moisture estimates, confirming initial suggestions by Bogena et al. (2013). Moreover, a strong correlation between biomass and the N_0 parameter was reported in several studies (Franz et al., 2013; Hawdon et al., 2014; Baatz et al., 2014, 2015). In our study, we pass the N_0 parameter as a calibration parameter set in mHM. In using the CRNS soil moisture measurement the drier locations show larger deviations than the wetter locations (Iwema et al., 2015). The possibility of using simulated high-resolution soil moisture profiles instead of a few measurements at different soil depths could further increase the accuracy of the model predictions (Brunetti et al., 2019). One of the primary sources of uncertainty at the *Grosses Bruch* site is surface ponding and shallow groundwater, as well as the loamy texture of the soil. Those factors contribute to the formation of permanent water ponds in the area and may introduce uniform or even inverse soil moisture profiles which directly influence the neutron emissions, but cannot be captured by the mHM model. Another factor is the time-variable effect of crowding cows near the station, which may influence the CRNS signal, but is challenging to correct in the CRNS measurement (Schrön et al., 2017). We incorporate the CRNS parameter set in mHM, and some parameters related

to soil moisture and neutron counts are effectively constrained based on the objective function using KGE$_{\alpha\beta}$. However, there is still room for improvement, particularly with regard to the coefficient in root fractions distributed across soil layers.

According to Beck et al. (2021), model calibration provides more overall benefits than data assimilation. Furthermore, model calibration can be advantageous for regions with both sparse and dense rain gauge networks, whereas data assimilation is more beneficial for regions with sparse rain gauge networks. In this paper, the Latin Hypercube Sampling (LHS) method McKay and Conover (1979) is adopted to generate input variable samples, which is a stratified sampling method that reduces the number of simulations required compared to the conventional Monte Carlo method Iman and Helton (1988). LHS divides the range of each input into N intervals and selects one representative value from each interval to ensure full coverage of the input variables range and representation of all possible values in the simulation. Previous studies by Smith et al. (2019) and Liu et al. (2022) addresses address the challenges of using the original KGE in Markov chain Monte Carlo (MCMC) methods, offering insights for accurate parameter estimation and posterior distribution exploration. To address this issue, it is recommended to use adaptations to the LHS method instead of directly using the original KGE to improve the exploration of the posterior distributions. Our approach can estimate the posterior distributions of model parameters based on the objective function KGE$_{\alpha\beta}$ by taking the variance and bias.

This paper provides a framework to incorporate CRNS data into the mHM to assess the accuracy of soil water content on different land cover types, including agricultural land, deciduous forest, and grassland. The integration of methods from Desilets et al. (2010) and Shuttleworth et al. (2013) in mHM, using climatic data and soil physical parameters, the parameterization of soil moisture and evapotranspiration can evapotranspiration is effectively improved (see Fig. ??). 9). Additionally, Supplementary Fig. S5 illustrates the improved representation of soil moisture for Hohes Holz. This framework lies in its ability to utilize observed neutron counts data, allowing for a comprehensive assessment of the model's performance and enhancing its reliability in hydrological modeling.
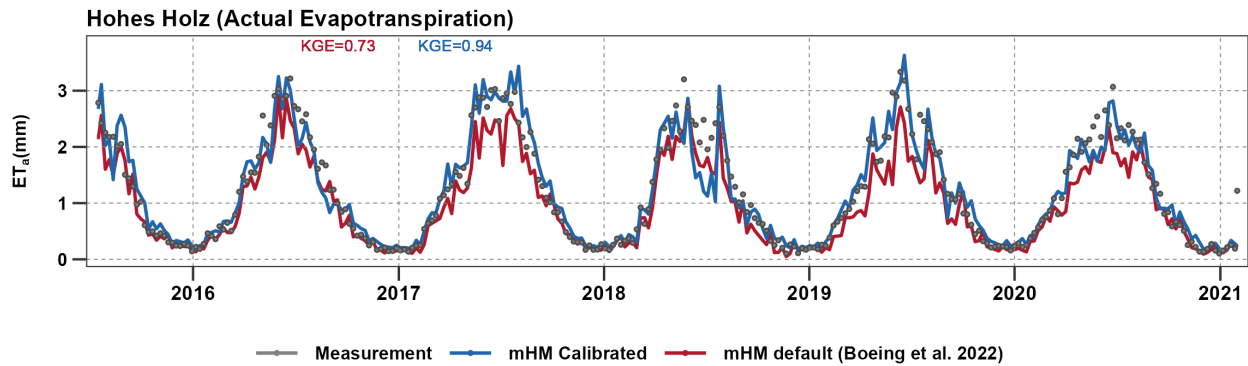
Figure 9. ~~(a)~~ Comparison of weekly ~~soil water content time series for 2014-2021 at a depth of 0-25 cm for *Hohes Holz* CRNS-based soil moisture data (grey line) and simulated data from mHM using two different sets of parameters. The red line represents the default parameters used in the German drought monitoring system as described by Boeing et al. (2022), while the blue line represents the best-calibrated value of our study with the improved Kling-Gupta Efficiency (KGE). (b) Comparison of weekly~~ observed actual evapotranspiration (grey dots) and simulated actual evapotranspiration using the default mHM parameters by Boeing et al. (2022) (red line) and the calibrated simulation (blue dots) over the *Hohes Holz* site.

~~The findings of this study suggest that, with certain cautionary notes, our method has the potential to better characterize drought compared to the approach used in the German drought monitoring system. Our assimilation of neutron counts in mHM resulted in more accurate predictions of soil water content compared to the approach described by Boeing et al. (2022) that is currently employed in the German drought monitor. However, the fact that our method still overestimated the severity of the drought in 2018 and 2019 is noticed, indicating that there may be other processes not accounted for by mHM that require further investigation.~~

5   Conclusion and future outlook

This study evaluates the potential of the mHM a large-scale hydrological model for simulating neutron counts at the ~~0.01562~~ 1.2 km ~~×0.01562grid~~ 1.2 km scale across different land cover sites for the period 2014–2021. Two empirical and one physical model approaches are evaluated for deriving neutrons from the soil moisture profile. Neutron measurement data from four sites in Germany are integrated, and the influence on hydrological model parameters, as well as simulated soil moisture and evapotranspiration are analyzed. The parameter sample of 100 000 realizations for neutron counts was taken, which are analyzed regarding their uncertainty caused by the parameter estimation. The parameter sets are filtered based on the KGE of observed vs simulated neutron counts. The best 1% member ensemble simulations are evaluated with neutron counts, evapotranspiration, and soil moisture observations.

The evaluation of neutron counts at four different sites ~~yield~~ yields a KGE value of > 0.8, indicating a satisfactory representation of the neutron observations. The 1% ensemble parameter set is found more representative of 100 000 realizations,

suggesting a reliable model performance. The performance of the neutron counting methods varies across different land cover types. The $N_{\text{Des,W}}$ method generally demonstrates good performance, particularly at the agricultural sites. While the N_{COSMIC} method performs slightly better at forest site and the $N_{\text{Des,U}}$ method shows slightly better results at the grassland site.

However, there is still room for improvement in some areas. Specifically, working with grassland sites presented challenges, particularly with the N_{COSMIC} method. On the one hand it is a physics-based approach incorporating a comprehensive representation of the neutron counting process, but on the other hand, it relies on the detailed representation of the site characteristics in the hydrological model. This complexity could introduce additional uncertainties and limitations in the model, potentially affecting its performance, especially when the site is more complex than it has been modeled. The study suggests that the observed discrepancies between model and observations may be attributed to the representation of dynamic biomass, snow, surface ponding, and shallow groundwater dynamics, which are present at the grassland site, for instance. Addressing these features could further enhance the model's accuracy.

The evaluation with evapotranspiration from eddy covariance at *Hohes Holz* stations indicates deficiencies in mHM to deal with forest systems, but also great potential for CRNS measurements to improve the water partitioning as a whole. Especially in the growing season (March-August), deviations of the modeled and observed ETa indicate room for better representation of mixed soils and dynamic vegetation modules at the local scale within mHM. The calibration on neutron counts not only improved the soil moisture performance of the model , but also helped to set the modeled evapotranspiration straight.

In conclusion, the incorporation of neutron counts estimation into mHM by accounting for vertical soil moisture profiles improves the model's accuracy and provides a more realistic representation of soil moisture dynamics ~~as well as evapotranspiration , particularly at the forest~~ at all four study sites and evapotranspiration at *Hohes Holz* site. This research presents a direction for future studies to explore. The next step in this research is to evaluate the ability of this CRNS module in mHM for estimating soil moisture through a large-scale soil moisture monitoring initiative, e.g. by utilizing more stationary CRNS networks or the novel rail-based CRNS data from Altdorff et al. (2023). To optimize accuracy and understanding, we recommend integrating both CRNS and satellite remote sensing data into mHM. Improving the model predictions will contribute to reducing the uncertainties associated with drought and flood management strategies and informed agricultural decisions.

Code availability. Simulation data is attached as supplemental material. The mesoscale Hydrological Model mHM (version 5.12) is open-source and can be freely accessed from GitLab: https://git.ufz.de/mhm/mhm/-/tree/v5.12.0?ref_type=tags.

Data availability. We kindly acknowledge the German Weather Service (DWD) for providing the meteorological datasets. The terrain elevation data was collected from USGS EROS Archive - Digital Elevation - Global Multi-resolution Terrain Elevation Data 2010 (GMTED2010), available at https://www.usgs.gov/centers/eros/science/usgs-eros-archive-digital-elevation-global-multi-resolution-terrain-elevation. Gridded soil characteristics are based on the BUEK200 database obtained from the German Federal Institute for Geosciences and Natural Resources (BGR, see online at https://geoportal.bgr.de/mapapps/resources/apps/geoportal/index.html?lang=en#/datasets/portal/154997F4-3C14-4A53-B217-8A7C7509E05F). The geological dataset was downloaded from Institute for Biogeochemistry and Marine

Chemistry, KlimaCampus, Universitt Hamburg (https://www.geo.uni-hamburg.de/en/geologie/forschung/aquatische-geochemie/glim.html). Leaf Area Index (LAI) dataset was downloaded from the Global Land Cover Facility (GLCF), available at http://iridl.ldeo.columbia.edu/ SOURCES/.UMD/.GLCF/.GIMMS/.NDVIg/.global/index.html. The land cover dataset was downloaded from the European Space Agency (ESA), available at http://due.esrin.esa.int/page_globcover.php. The ET data were obtained from https://zenodo.org/record/7561854.

630 *Competing interests.* RK and LS are members of the editorial board of Hydrology and Earth System Sciences.

Acknowledgements. The authors thank all the site owners for maintaining the local sensors, particularly to F. Böttcher (DWD) and E. Thiel (SKWP). The study has been made possible by the Terrestrial Environmental Observatories (TERENO), an infrastructural fund of the Helmholtz Association. The High-Performance Computing Cluster EVE has contributed to the computation of the scientific findings. Eshrat Fatima is grateful for the financial support of the German Academic Exchange Service (DAAD) through the Graduate School Scholarship
635 Program under Reference Number 91788160.

References

Albergel, C., Calvet, J.-C., Rosnay, P. d., Balsamo, G., Wagner, W., Hasenauer, S., Naeimi, V., Martin, E., Bazile, E., Bouyssel, F., et al.: Cross-evaluation of modelled and remotely sensed surface soil moisture with in situ data in southwestern France, Hydrology and Earth System Sciences, 14, 2177–2191, 2010.

640 Altdorff, D., Oswald, S. E., Zacharias, S., Zengerle, C., Dietrich, P., Mollenhauer, H., Attinger, S., and Schrön, M.: Toward Large-Scale Soil Moisture Monitoring Using Rail-Based Cosmic Ray Neutron Sensing, Water Resources Research, 59, e2022WR033 514, 2023.

Andreasen, M., Jensen, K. H., Desilets, D., Franz, T. E., Zreda, M., Bogena, H. R., and Looms, M. C.: Status and perspectives on the cosmic-ray neutron method for soil moisture estimation and other environmental science applications, Vadose Zone Journal, 16, 1–11, 2017.

645 Avery, W. A., Finkenbiner, C., Franz, T. E., Wang, T., Nguy-Robertson, A. L., Suyker, A., Arkebauer, T., and Muñoz Arriola, F.: Incorporation of globally available datasets into the roving cosmic-ray neutron probe method for estimating field-scale soil water content, Hydrology and Earth System Sciences, 20, 3859–3872, https://doi.org/10.5194/hess-20-3859-2016, 2016.

Baatz, R., Bogena, H., Franssen, H.-J. H., Huisman, J., Qu, W., Montzka, C., and Vereecken, H.: Calibration of a catchment scale cosmic-ray probe network: A comparison of three parameterization methods, Journal of Hydrology, 516, 231–244, 2014.

650 Baatz, R., Bogena, H., Hendricks Franssen, H.-J., Huisman, J., Montzka, C., and Vereecken, H.: An empirical vegetation correction for soil water content quantification using cosmic ray probes, Water Resources Research, 51, 2030–2046, 2015.

Baatz, R., Hendricks Franssen, H.-J., Han, X., Hoar, T., Bogena, H. R., and Vereecken, H.: Evaluation of a cosmic-ray neutron sensor network for improved land surface model prediction, Hydrology and Earth System Sciences, 21, 2509–2530, 2017.

Barbosa, L. R., Coelho, V. H. R., Scheiffele, L. M., Baroni, G., Ramos Filho, G. M., Montenegro, S. M., Almeida, C. d. N., and Oswald,
655 S. E.: Dynamic groundwater recharge simulations based on cosmic-ray neutron sensing in a tropical wet experimental basin, Vadose Zone Journal, 20, e20 145, 2021.

Baroni, G. and Oswald, S.: A scaling approach for the assessment of biomass changes and rainfall interception using cosmic-ray neutron sensing, Journal of Hydrology, 525, 264–276, 2015.

Beck, H. E., Pan, M., Miralles, D. G., Reichle, R. H., Dorigo, W. A., Hahn, S., Sheffield, J., Karthikeyan, L., Balsamo, G., Parinussa, R. M.,
660 et al.: Evaluation of 18 satellite-and model-based soil moisture products using in situ measurements from 826 sensors, Hydrology and Earth System Sciences, 25, 17–40, 2021.

BGR: Digital soil map of Germany 1 : 200,000 (BUEK 200) v0.5, https://www.bgr.bund.de/DE/Themen/Boden/Informationsgrundlagen/Bodenkundliche_Karten_Datenbanken/BUEK200/buek200_node.html, [Accessed: October 7, 2022], 2020.

Boeing, F., Rakovec, O., Kumar, R., Samaniego, L., Schrön, M., Hildebrandt, A., Rebmann, C., Thober, S., Müller, S., Zacharias, S., Bogena,
665 H., Schneider, K., Kiese, R., Attinger, S., and Marx, A.: High-resolution drought simulations and comparison to soil moisture observations in Germany, Hydrology and Earth System Sciences, 26, 5137–5161, https://doi.org/10.5194/hess-26-5137-2022, 2022.

Bogena, H., Huisman, J., Baatz, R., Hendricks Franssen, H.-J., and Vereecken, H.: Accuracy of the cosmic-ray soil water content probe in humid forest ecosystems: The worst case scenario, Water Resources Research, 49, 5778–5791, 2013.

Bogena, H. R., Schrön, M., Jakobi, J., Ney, P., Zacharias, S., Andreasen, M., Baatz, R., Boorman, D., Duygu, M. B., Eguibar-Galán, M. A.,
670 et al.: COSMOS-Europe: a European network of cosmic-ray neutron soil moisture sensors, Earth System Science Data, 14, 1125–1151, 2022.

Brunetti, G., Bogena, H., Baatz, R., Huisman, J. A., Dahlke, H., and Vereecken, H.: On the information content of cosmic-ray neutron data in the inverse estimation of soil hydraulic properties, Vadose Zone Journal, 18, 1–24, 2019.

Chan, S. K., Bindlish, R., O'Neill, P., Jackson, T., Njoku, E., Dunbar, S., Chaubell, J., Piepmeier, J., Yueh, S., Entekhabi, D., et al.: Development and assessment of the SMAP enhanced passive soil moisture product, Remote sensing of environment, 204, 931–941, 2018.

Chen, F., Crow, W. T., Starks, P. J., and Moriasi, D. N.: Improving hydrologic predictions of a catchment model via assimilation of surface soil moisture, Advances in Water Resources, 34, 526–536, 2011.

Desilets, D., Zreda, M., and Ferré, T. P.: Nature's neutron probe: Land surface hydrology at an elusive scale with cosmic rays, Water Resources Research, 46, 2010.

Dimitrova-Petrova, K., Geris, J., Wilkinson, M. E., Rosolem, R., Verrot, L., Lilly, A., and Soulsby, C.: Opportunities and challenges in using catchment-scale storage estimates from cosmic ray neutron sensors for rainfall-runoff modelling, Journal of Hydrology, 586, 124 878, 2020.

Dong, J. and Ochsner, T. E.: Soil texture often exerts a stronger influence than precipitation on mesoscale soil moisture patterns, Water Resources Research, 54, 2199–2211, 2018.

Dong, J., Ochsner, T. E., Zreda, M., Cosh, M. H., and Zou, C. B.: Calibration and validation of the COSMOS rover for surface soil moisture measurement, Vadose Zone Journal, 13, 1–8, 2014.

Döpper, V., Rocha, A. D., Berger, K., Gränzig, T., Verrelst, J., Kleinschmit, B., and Förster, M.: Estimating soil moisture content under grassland with hyperspectral data using radiative transfer modelling and machine learning, International Journal of Applied Earth Observation and Geoinformation, 110, 102 817, 2022.

ESA: Global Land Cover Map for 2009, http://due.esrin.esa.int/files/Globcover2009_V2.3_Global_.zip, last accessed on 1 June 2021, 2009.

Foolad, F., Franz, T. E., Wang, T., Gibson, J., Kilic, A., Allen, R. G., and Suyker, A.: Feasibility analysis of using inverse modeling for estimating field-scale evapotranspiration in maize and soybean fields from soil water content monitoring networks, Hydrology and Earth System Sciences, 21, 1263–1277, https://doi.org/10.5194/hess-21-1263-2017, 2017.

Franz, T., Zreda, M., Rosolem, R., and Ferre, T.: A universal calibration function for determination of soil moisture with cosmic-ray neutrons, Hydrology and Earth System Sciences, 17, 453–460, 2013.

Franz, T. E., Zreda, M., Ferre, T., Rosolem, R., Zweck, C., Stillman, S., Zeng, X., and Shuttleworth, W.: Measurement depth of the cosmic ray soil moisture probe affected by hydrogen from various sources, Water Resources Research, 48, 2012a.

Franz, T. E., Zreda, M., Rosolem, R., and Ferre, T.: Field Validation of a Cosmic-Ray Neutron Sensor Using a Distributed Sensor Network, Vadose Zone Journal, 11, https://doi.org/10.2136/vzj2012.0046, 2012b.

Franz, T. E., Wahbi, A., Zhang, J., Vreugdenhil, M., Heng, L., Dercon, G., Strauss, P., Brocca, L., and Wagner, W.: Practical data products from cosmic-ray neutron sensing for hydrological applications, Frontiers in Water, 2, 9, 2020.

Fuamba, M., Branger, F., Braud, I., Batchabani, E., Sanzana, P., Sarrazin, B., and Jankowfsky, S.: Value of distributed water level and soil moisture data in the evaluation of a distributed hydrological model: Application to the PUMMA model in the Mercier catchment (6.6 km2) in France, Journal of Hydrology, 569, 753–770, 2019.

Greacen, E. L.: Soil water assessment by the neutron method, CSIRO, Australia, 1981.

Gupta, H. V., Sorooshian, S., and Yapo, P. O.: Status of automatic calibration for hydrologic models: Comparison with multilevel expert calibration, Journal of hydrologic engineering, 4, 135–143, 1999.

Gupta, H. V., Kling, H., Yilmaz, K. K., and Martinez, G. F.: Decomposition of the mean squared error and NSE performance criteria: Implications for improving hydrological modelling, Journal of Hydrology, 377, 80–91, 2009.

Hargreaves, G. H. and Samani, Z. A.: Reference Crop Evapotranspiration from Temperature, Applied Engineering in Agriculture, 1, 96–99, https://doi.org/10.13031/2013.26773, 1985.

Hawdon, A., McJannet, D., and Wallace, J.: Calibration and correction procedures for cosmic-ray neutron soil moisture probes located across Australia, Water Resources Research, 50, 5029–5043, 2014.

Hermanns, F., Pohl, F., Rebmann, C., Schulz, G., Werban, U., and Lausch, A.: Inferring grassland drought stress with unsupervised learning from airborne hyperspectral VNIR imagery, Remote Sensing, 13, 1885, 2021.

Iman, R. L. and Helton, J. C.: An investigation of uncertainty and sensitivity analysis techniques for computer models, Risk analysis, 8, 71–90, 1988.

Iwema, J., Rosolem, R., Baatz, R., Wagener, T., and Bogena, H.: Investigating temporal field sampling strategies for site-specific calibration of three soil moisture–neutron intensity parameterisation methods, Hydrology and Earth System Sciences, 19, 3203–3216, 2015.

Iwema, J., Rosolem, R., Rahman, M., Blyth, E., and Wagener, T.: Land surface model performance using cosmic-ray and point-scale soil moisture measurements for calibration, Hydrology and Earth System Sciences, 21, 2843–2861, 2017.

Iwema, J., Schrön, M., Koltermann Da Silva, J., Schweiser De Paiva Lopes, R., and Rosolem, R.: Accuracy and precision of the cosmic-ray neutron sensor for soil moisture estimation at humid environments, Hydrological Processes, 35, e14 419, 2021.

Jablonowski, C.: Adaptive grids in weather and climate modeling, University of Michigan, 2004.

James, L. D.: Selection, calibration, and testing of hydrologic models, Hydrologic modeling of small watersheds, pp. 437–472, 1982.

Kasner, M., Zacharias, S., and Schrön, M.: On soil bulk density and its influence to soil moisture estimation with cosmic-ray neutrons, Hydrology and Earth System Sciences Discussions, pp. 1–24, 2022.

Köhli, M., Schrön, M., Zreda, M., Schmidt, U., Dietrich, P., and Zacharias, S.: Footprint characteristics revised for field-scale soil moisture monitoring with cosmic-ray neutrons, Water Resources Research, 51, 5772–5790, 2015.

Kumar, R., Livneh, B., and Samaniego, L.: Toward computationally efficient large-scale hydrologic predictions with a multiscale regionalization scheme, Water Resources Research, 49, 5700–5714, 2013a.

Kumar, R., Samaniego, L., and Attinger, S.: Implications of distributed hydrologic model parameterization on water fluxes at multiple scales and locations, Water Resources Research, 49, 360–379, 2013b.

Kvålseth, T. O.: Cautionary note about R 2, The American Statistician, 39, 279–285, 1985.

Köhli, M., Weimar, J., Schrön, M., Baatz, R., and Schmidt, U.: Soil Moisture and Air Humidity Dependence of the Above-Ground Cosmic-Ray Neutron Intensity, Frontiers in Water, 2, 544 847, https://doi.org/10.3389/frwa.2020.544847, 2021.

Liu, Y., Fernández-Ortega, J., Mudarra, M., and Hartmann, A.: Pitfalls and a feasible solution for using KGE as an informal likelihood function in MCMC methods: DREAM (ZS) as an example, Hydrology and Earth System Sciences, 26, 5341–5355, 2022.

Livneh, B., Kumar, R., and Samaniego, L.: Influence of soil textural properties on hydrologic fluxes in the Mississippi river basin, Hydrological Processes, 29, 4638–4655, 2015.

Mai, J.: Ten strategies towards successful calibration of environmental models, Journal of Hydrology, p. 129414, https://doi.org/10.1016/j.jhydrol.2023.129414, 2023.

Martinez, G. F. and Gupta, H. V.: Toward improved identification of hydrological models: A diagnostic evaluation of the "abcd" monthly water balance model for the conterminous United States, Water Resources Research, 46, 2010.

Massoud, E. C., Xu, C., Fisher, R. A., Knox, R. G., Walker, A. P., Serbin, S. P., Christoffersen, B. O., Holm, J. A., Kueppers, L. M., Ricciuto, D. M., et al.: Identification of key parameters controlling demographically structured vegetation dynamics in a land surface model: CLM4. 5 (FATES), Geoscientific Model Development, 12, 4133–4164, 2019.

McKay, M. and Conover, W.: RJ Beckman A comparison of three methods for selecting values of input variables in the analysis of output from a computer code, Technometrics, 21, 239–245, 1979.

750 Nash, J. E. and Sutcliffe, J. V.: River flow forecasting through conceptual models part I—A discussion of principles, Journal of Hydrology, 10, 282–290, 1970.

OpenStreetMap contributors: Planet dump retrieved from https://planet.osm.org (last access: 26 July 2021), available at: https://www.openstreetmap.org (last access: 26 July 2021), a, b, c, 2020.

Orth, R., Staudinger, M., Seneviratne, S. I., Seibert, J., and Zappa, M.: Does model performance improve with complexity? A case study 755 with three hydrological models, Journal of Hydrology, 523, 147–159, 2015.

Patil, A., Fersch, B., Hendricks Franssen, H.-J., and Kunstmann, H.: Assimilation of cosmogenic neutron counts for improved soil moisture prediction in a distributed land surface model, Frontiers in Water, p. 115, 2021.

Pohl, F., Rakovec, O., Rebmann, C., Hildebrandt, A., Boeing, F., Hermanns, F., Attinger, S., Samaniego, L., and Kumar, R.: Long-term daily hydrometeorological drought indices, soil moisture, and evapotranspiration for ICOS sites, Scientific Data, 10, 281, 2023.

760 Rakovec, O., Kumar, R., Attinger, S., and Samaniego, L.: Improving the realism of hydrologic model functioning through multivariate parameter estimation, Water Resources Research, 52, 7779–7792, 2016.

Rivera Villarreyes, C., Baroni, G., and Oswald, S. E.: Integral quantification of seasonal soil moisture changes in farmland by cosmic-ray neutrons, Hydrology and Earth System Sciences, 15, 3843–3859, 2011.

Rivera Villarreyes, C. A., Baroni, G., and Oswald, S. E.: Inverse modelling of cosmic-ray soil moisture for field-scale soil hydraulic param- 765 eters, European Journal of Soil Science, 65, 876–886, https://doi.org/10.1111/ejss.12162, 2014.

Rosolem, R., Hoar, T., Arellano, A., Anderson, J. L., Shuttleworth, W. J., Zeng, X., and Franz, T. E.: Translating aboveground cosmic-ray neutron intensity to high-frequency soil moisture profiles at sub-kilometer scale, Hydrology and Earth System Sciences, 18, 4363–4379, 2014.

Samaniego, L., Bárdossy, A., and Kumar, R.: Streamflow prediction in ungauged catchments using copula-based dissimilarity measures, 770 Water Resources Research, 46, 2010a.

Samaniego, L., Kumar, R., and Attinger, S.: Multiscale parameter regionalization of a grid-based hydrologic model at the mesoscale, Water Resources Research, 46, 2010b.

Samaniego, L., Kumar, R., Thober, S., Rakovec, O., Zink, M., Wanders, N., Eisner, S., Müller Schmied, H., Sutanudjaja, E. H., Warrach-Sagi, K., et al.: Toward seamless hydrologic predictions across spatial scales, Hydrology and Earth System Sciences, 21, 4323–4346, 2017.

775 Samaniego, L., Thober, S., Wanders, N., Pan, M., Rakovec, O., Sheffield, J., Wood, E. F., Prudhomme, C., Rees, G., Houghton-Carr, H., Fry, M., Smith, K., Watts, G., Hisdal, H., Estrela, T., Buontempo, C., Marx, A., and Kumar, R.: Hydrological Forecasts and Projections for Improved Decision-Making in the Water Sector in Europe, Bulletin of the American Meteorological Society, 100, 2451–2472, https://doi.org/10.1175/bams-d-17-0274.1, 2019.

Samaniego, L., Kumar, R., Zink, M., Cuntz, M., Mai, J., Thober, S., Schneider, C., Dalmasso, G., Musuuza, J., Rakovec, O., Craven, 780 J., Schäfer, D., Prykhodko, V., Schrön, M., Spieler, D., Brenner, J., Langenberg, B., Schüler, L., Stisen, S., Demirel, C. M., Jing, M., Kaluza, M., Schweppe, R., Shrestha, P. K., Döring, N., and Müller, S.: mesoscale Hydrologic Model - mHM v5.13.0, Zenodo, https://doi.org/10.5281/zenodo.7997974, 2023.

Santanello Jr, J. A., Peters-Lidard, C. D., and Kumar, S. V.: Diagnosing the sensitivity of local land–atmosphere coupling via the soil moisture–boundary layer interaction, Journal of Hydrometeorology, 12, 766–786, 2011.

Schreiner-McGraw, A. P., Vivoni, E. R., Mascaro, G., and Franz, T. E.: Closing the water balance with cosmic-ray soil moisture measurements and assessing their relation to evapotranspiration in two semiarid watersheds, Hydrology and Earth System Sciences, 20, 329–345, https://doi.org/10.5194/hess-20-329-2016, 2015.

Schreiner-McGraw, A. P., Vivoni, E. R., Mascaro, G., and Franz, T. E.: Closing the water balance with cosmic-ray soil moisture measurements and assessing their relation to evapotranspiration in two semiarid watersheds, Hydrology and Earth System Sciences, 20, 329–345, 2016.

Schrön, M.: Cosmic-ray Neutron Sensing and Its Applications to Soil and Land Surface Hydrology: On Neutron Physics, Method Development, and Soil Moisture Estimation Across Scales, Ph.D. thesis, Universität Potsdam, https://publishup.uni-potsdam.de/files/39543/schroen_diss.pdf, 2017.

Schrön, M., Köhli, M., Scheiffele, L., Iwema, J., Bogena, H. R., Lv, L., Martini, E., Baroni, G., Rosolem, R., Weimar, J., et al.: Improving calibration and validation of cosmic-ray neutron sensors in the light of spatial sensitivity, Hydrology and Earth System Sciences, 21, 5009–5030, 2017.

Schrön, M., Oswald, S. E., Zacharias, S., Kasner, M., Dietrich, P., and Attinger, S.: Neutrons on rails: Transregional monitoring of soil moisture and snow water equivalent, Geophysical research letters, 48, e2021GL093 924, 2021.

Seneviratne, S. I., Lüthi, D., Litschi, M., and Schär, C.: Land–atmosphere coupling and climate change in Europe, Nature, 443, 205–209, 2006.

Shuttleworth, J., Rosolem, R., Zreda, M., and Franz, T.: The COsmic-ray Soil Moisture Interaction Code (COSMIC) for use in data assimilation, Hydrology and Earth System Sciences, 17, 3205–3217, 2013.

Smith, K. A., Barker, L. J., Tanguy, M., Parry, S., Harrigan, S., Legg, T. P., Prudhomme, C., and Hannaford, J.: A multi-objective ensemble approach to hydrological modelling in the UK: an application to historic drought reconstruction, Hydrology and Earth System Sciences, 23, 3247–3268, 2019.

Van Steenbergen, N. and Willems, P.: Increasing river flood preparedness by real-time warning based on wetness state conditions, Journal of Hydrology, 489, 227–237, 2013.

Vather, T., Everson, C., and Franz, T. E.: Calibration and validation of the cosmic ray neutron rover for soil water mapping within two South African land classes, Hydrology, 6, 65, 2019.

Viviroli, D., Zappa, M., Gurtz, J., and Weingartner, R.: An introduction to the hydrological modelling system PREVAH and its pre-and post-processing-tools, Environmental Modelling & Software, 24, 1209–1222, 2009.

Wahbi, A., Heng, L., and Dercon, G.: Cosmic ray neutron sensing: estimation of agricultural crop biomass water equivalent, Springer Nature, 2018.

Wang, E., Smith, C. J., Macdonald, B. C., Hunt, J. R., Xing, H., Denmead, O., Zeglin, S., Zhao, Z., and Isaac, P.: Making sense of cosmic-ray soil moisture measurements and eddy covariance data with regard to crop water use and field water balance, Agricultural Water Management, 204, 271–280, https://doi.org/10.1016/j.agwat.2018.04.017, 2018.

Warm Winter, W.: Warm Winter 2020 Team and ICOS Ecosystem Thematic Centre: Warm Winter 2020 ecosystem eddy covariance flux product for 73 stations in FLUXNET-Archive format–release 2022-1 (Version 1.0), ICOS Carbon Portal [data set], https://doi.org/10.18160/2G60-ZHAK, 2022.

Wollschläger, U., Attinger, S., Borchardt, D., Brauns, M., Cuntz, M., Dietrich, P., Fleckenstein, J. H., Friese, K., Friesen, J., Harpke, A., et al.: The Bode hydrological observatory: a platform for integrated, interdisciplinary hydro-ecological research within the TERENO Harz/Central German Lowland Observatory, Environmental Earth Sciences, 76, 1–25, 2017.

Zacharias, S. and Wessolek, G.: Excluding organic matter content from pedotransfer predictors of soil water retention, Soil Science Society of America Journal, 71, 43–50, 2007.

Zacharias, S., Bogena, H., Samaniego, L., Mauder, M., Fuß, R., Pütz, T., Frenzel, M., Schwank, M., Baessler, C., Butterbach-Bahl, K., et al.: A network of terrestrial environmental observatories in Germany, Vadose zone journal, 10, 955–973, 2011.

Zhao, H., Montzka, C., Baatz, R., Vereecken, H., and Franssen, H.-J. H.: The Importance of Subsurface Processes in Land Surface Modeling over a Temperate Region: An Analysis with SMAP, Cosmic Ray Neutron Sensing and Triple Collocation Analysis, Remote Sensing, 13, 3068, 2021.

Zhuo, L., Dai, Q., Zhao, B., and Han, D.: Soil moisture sensor network design for hydrological applications, Hydrology and Earth System Sciences, 24, 2577–2591, 2020.

Zink, M., Kumar, R., Cuntz, M., and Samaniego, L.: A high-resolution dataset of water fluxes and states for Germany accounting for parametric uncertainty, Hydrology and Earth System Sciences, 21, 1769–1790, 2017.

Zreda, M.: Land-surface hydrology with cosmic-ray neutrons: Principles and applications, Journal of the Japanese Society of Soil Physics, 132, 25–30, 2016.

Zreda, M., Desilets, D., Ferré, T., and Scott, R. L.: Measuring soil moisture content non-invasively at intermediate spatial scale using cosmic-ray neutrons, Geophysical research letters, 35, 2008.

Zreda, M., Shuttleworth, W., Zeng, X., Zweck, C., Desilets, D., Franz, T., and Rosolem, R.: COSMOS: The cosmic-ray soil moisture observing system, Hydrology and Earth System Sciences, 16, 4079–4099, 2012a.

Zreda, M., Shuttleworth, W. J., Zeng, X., Zweck, C., Desilets, D., Franz, T., and Rosolem, R.: COSMOS: the COsmic-ray Soil Moisture Observing System, Hydrology and Earth System Sciences, 16, 4079–4099, https://doi.org/10.5194/hess-16-4079-2012, 2012b.